

# THE EVOLUTION OF EARLY-TYPE GALAXIES IN DISTANT CLUSTERS<sup>1</sup>

S. A. STANFORD<sup>2,3</sup>

Institute of Geophysics and Planetary Physics, Lawrence Livermore National Laboratory, Livermore, CA 94550; adam@igpp.llnl.gov

PETER R. EISENHARDT<sup>3</sup>

Jet Propulsion Laboratory, California Institute of Technology, Pasadena, CA 91109; prme@kromos.jpl.nasa.gov

AND

MARK DICKINSON<sup>3,4</sup>

Department of Physics and Astronomy, The Johns Hopkins University, Baltimore, MD 21218; med@stsci.edu

Received 1996 December 23; accepted 1997 August 18

## ABSTRACT

We present results from an optical–infrared photometric study of early-type (E+S0) galaxies in 19 galaxy clusters out to  $z = 0.9$ . The galaxy sample is selected on the basis of morphologies determined from *Hubble Space Telescope* (HST) WFPC2 images and is photometrically defined in the  $K$  band in order to minimize redshift-dependent selection biases. Using new ground-based photometry in five optical and infrared bands for each cluster, we examine the evolution of the color–magnitude relation for early-type cluster galaxies, considering its slope, intercept, and color scatter around the mean relation. New multiwavelength photometry of galaxies in the Coma Cluster is used to provide a baseline sample at  $z \approx 0$  with which to compare the distant clusters. The optical–IR colors of the early-type cluster galaxies become bluer with increasing redshift in a manner consistent with the passive evolution of an old stellar population formed at an early cosmic epoch. The degree of color evolution is similar for clusters at similar redshift and does not depend strongly on the optical richness or X-ray luminosity of the cluster, which suggests that the history of early-type galaxies is relatively insensitive to environment, at least above a certain density threshold. The slope of the color–magnitude relationship shows no significant change out to  $z = 0.9$ , which provides evidence that it arises from a correlation between galaxy mass and metallicity, not age. Finally, the intrinsic scatter in the optical–IR colors of the galaxies is small and nearly constant with redshift, which indicates that the majority of giant, early-type galaxies in clusters share a common star formation history, with little perturbation due to uncorrelated episodes of later star formation. Taken together, our results are consistent with models in which most early-type galaxies in rich clusters are old, formed the majority of their stars at high redshift in a well-synchronized fashion, and evolved quiescently thereafter. We consider several possible effects that may be introduced by the choice of morphologically recognizable elliptical and S0 galaxies in dense environments as a subject for study. In particular, the inclusion of S0 galaxies, which might be undergoing morphological transformation in clusters as part of the Butcher–Oemler effect, may influence the results of our investigation.

*Subject headings:* galaxies: clusters: general — galaxies: elliptical and lenticular, cD — galaxies: evolution — galaxies: photometry

## 1. INTRODUCTION

The elliptical galaxy formation scenario proposed by, e.g., Eggen, Lynden-Bell, & Sandage (1962; hereafter ELS), Searle, Sargent, & Bagnuolo (1973), and Tinsley & Gunn (1976) postulates a single burst of star formation at high redshift, followed by passive stellar evolution. An elliptical galaxy is assumed to form the vast majority of its stellar mass during the initial starburst. Several observations suggest that early-type galaxies in present-day clusters may have formed and evolved in this fashion. For example, the

color–magnitude ( $C-M$ ) relation seen in nearby clusters can be readily explained in terms of a single star formation episode. More massive galaxies would retain supernovae ejecta more effectively, resulting in higher metallicities for the succeeding generations of stars within the initial burst and hence in redder colors for more luminous galaxies (Larson 1974; Arimoto & Yoshii 1987; Franx & Illingworth 1990). Indeed, the  $C-M$  relation in nearby clusters evidently implies a close tie between metallicity and galaxy mass, as seen in the tightness of the  $Mg_2-\sigma$  correlation (Bender, Burstein, & Faber 1993). Furthermore, the scatter in the  $UVK$  colors of present-epoch cluster E+S0 galaxies is observed to be very small (Bower, Lucey, & Ellis 1992; Eisenhardt et al. 1998). This has been used to argue for a high degree of synchronization in their star formation histories and for relatively old ages. Late, episodic bursts of star formation, young galaxy ages, or a wide range in galaxy formation redshifts would be expected to lead to larger color scatter than is observed. An early formation epoch coupled with passive evolution simply predicts the observed homogeneity in the colors of most elliptical galaxies in clusters today.

<sup>1</sup> Based on observations made with the NASA/ESA Hubble Space Telescope, obtained from the data archive and at the Space Telescope Science Institute, which is operated by the Association of Universities for Research in Astronomy, Inc., under cooperative agreement with the National Science Foundation.

<sup>2</sup> Jet Propulsion Laboratory, California Institute of Technology.

<sup>3</sup> Visiting Astronomer, Kitt Peak National Observatory, National Optical Astronomy Observatories, which is operated by the Association of Universities for Research in Astronomy, Inc., under cooperative agreement with the National Science Foundation.

<sup>4</sup> Alan C. Davis Fellow, also with the Space Telescope Science Institute.

There is, however, spectroscopic evidence for younger stellar populations in some elliptical and S0 galaxies (O'Connell 1980; Worthey 1996), as well as morphological signs of disturbance attributed to past merger events (Toomre 1978; Schweizer & Seitzer 1988). Moreover, Schweizer et al. (1990) and Schweizer & Seitzer (1992) have shown that the spectroscopic and photometric indicators of younger starlight correlate with the degree of morphological disturbance in E and S0 galaxies, which implies a connection between the two phenomena. The galaxy samples considered in such studies have consisted primarily of *field* galaxies and have not included galaxies in the cores of rich clusters such as Coma. It is therefore unclear whether these results apply to all early-type galaxies or are a function of their environment.

The traditional picture of massive galaxy formation in a monolithic collapse episode at high redshift does not sit comfortably within the context of modern hierarchical merging scenarios for galaxy formation and evolution, such as those based on the cold dark matter (CDM) model. Such models predict that massive galaxies form late, at  $z \leq 2$ , from the gradual merging of smaller galaxies (see, e.g., White & Frenk 1991; Kauffmann, White, & Guideroni 1993; Cole et al. 1994). Although this scenario predicts a wide range of ages for elliptical galaxies, their small color scatter in the present epoch can be accommodated because sufficient time elapses since the epoch of extensive merging for the resulting color variations to damp out (Kauffmann 1996; see also Schweizer & Seitzer 1992). The mass-metallicity correlation implied by the slope of the color-magnitude relation has been recently examined in the context of hierarchical merging models by Kauffmann & Charlot (1997). Using a multimetallicity spectral synthesis code and semianalytical galaxy evolution models, they are able to reproduce this correlation by forming more massive ellipticals from mergers of more massive progenitor disk galaxies, which themselves are better able to retain metals during star formation.

The aforementioned observational constraints on E/S0 galaxies are well known only at  $z = 0$ , which allows a wide range of possible star formation histories, including both the ELS and CDM scenarios. Recent observational advances both on the ground and in space are beginning to provide detailed information on the properties of early-type galaxies at higher redshift, e.g., through study of the fundamental plane and its projections (Dokkum & Franx 1996; Dickinson 1995, 1997; Pahre, Djorgovski, & De Carvalho 1996) and the Mg- $\sigma$  relation (Ziegler & Bender 1997). By examining the properties of galaxies in clusters at high redshifts, constraints on the nature of early-type galaxy evolution might be developed so as to favor one formation scenario over the other.

In practice, several complications have arisen in investigations of galaxy evolution in distant clusters. Photometric studies based on optical imaging (see, e.g., Butcher & Oemler 1978; Dressler & Gunn 1992; Rakos & Schombert 1995; and Lubin 1996) may be hampered by selection effects due to the redshifting of blue and ultraviolet rest-frame wavelengths into the observed bands. This is a significant concern for galaxy selection in the most distant known clusters from optical and X-ray samples ( $z \approx 0.9$ ), where even the *I*-band measures blue wavelengths in the cluster rest frame. Selecting galaxy samples in the near-infrared alleviates this problem. Even at  $z \sim 1$ , the *K* band measures

galaxy light emitted in the rest-frame near-IR. Because the infrared spectral energy distributions of all but the most vigorously star-forming galaxies are very similar (see, e.g., Johnson 1966), a galaxy sample defined in the near-IR should be free of redshift-dependent biases regarding galaxy type out to  $z \approx 1$  and beyond. Optical-to-infrared photometry, particularly where the optical band measures light emitted shortward of 4000 Å in the rest frame, ensures a long-wavelength baseline for color measurements, providing in effect a measurement of the luminosity ratio of main-sequence stars to evolved red giants in a galaxy's stellar population (see, e.g., Bruzual & Charlot 1993). Aragón-Salamanca et al. (1993) used this approach to study color evolution in a study of  $10 \geq z \geq 0.5$  clusters and found that the modal optical-IR colors of the galaxies, presumed to be primarily cluster ellipticals, become bluer with redshift.

Without the ability to distinguish between morphological classes of galaxies in distant clusters, purely ground-based photometric studies run the risk of mixing galaxy types. This results in a particular hazard for studying the evolution of early-type galaxies, since the increasing proportion of blue, late-type galaxies in distant clusters (the "Butcher-Oemler effect") may introduce greater contamination at higher redshifts. Imaging data from the *Hubble Space Telescope* (*HST*) largely solves this problem by providing the capability to select galaxies purely by morphology (Dressler et al. 1994; Couch et al. 1994). In Stanford, Eisenhardt, & Dickinson (1995; hereafter SED95), we made a first attempt to combine multiband optical-IR photometry with *HST* imaging of two clusters to evaluate the evolutionary state of early-type cluster galaxies at  $z \approx 0.4$ . In that paper, the rest-frame *V*–*H* colors of distant, morphologically selected early-type galaxies were found to be similar ( $< 0.2$  mag bluer) to those at  $z = 0$ , and the slope and scatter of the color-magnitude relation for those galaxies were also found to be indistinguishable from the present-day values. Ellis et al. (1997) have recently made a similar test using multicolor optical WFPC2 data to study E + S0 galaxies in three clusters at  $z \approx 0.54$ , with similar results.

In the present paper, we extend the analysis of SED95 to a much larger sample of galaxy clusters, spanning a wide redshift range ( $0 < z < 0.9$ ), using substantially improved optical-IR photometric data. For  $\Lambda = 0$  cosmologies with  $0.05 < q_0 < 0.5$ , our cluster sample spans 50%–62% of the look-back time to the big bang, affording us a broad view of the evolution of early-type galaxies throughout the second half of the universe's lifespan. Our major results are presented here; the photometric data set itself will be presented in a supplemental paper (Stanford et al. 1998). Except where noted, the assumed cosmology is  $H_0 = 65 \text{ km s}^{-1} \text{ Mpc}^{-1}$ ,  $q_0 = 0.05$ , and  $\Lambda = 0$ , which results in a present-day age for the universe of 13.5 Gyr.

In this paper, we use the term "early-type" galaxy to refer to those galaxies classified morphologically as having Hubble classes E, E/S0, or S0. We have made no attempt here to subdivide further the early-type galaxy population into high-redshift clusters, and in particular no effort has been made to separate elliptical from S0 galaxies. Making such morphological distinctions is sometimes difficult even for nearby galaxies and is dependent on orientation: a face-on S0 galaxy, for example, can be hard to distinguish from a "true" elliptical galaxy. It has yet to be established how well this subclassification can be achieved for WFPC2 images of high-redshift galaxies (see Smail et al. 1997 for a

discussion), and for the purposes of this paper we have preferred to avoid the resulting uncertainties which might arise from misclassification. However, grouping elliptical and S0 galaxies together for an evolutionary study such as this one may have undesirable consequences for the interpretation of the results. We will return to this point in § 4. Throughout the text, except where we wish to make the distinction between elliptical and S0 galaxies explicit, we will generally use the terms “early-type” and E+S0 interchangeably to refer to the overall population of elliptical and S0 galaxies in a cluster.

In addition, we note here that the subject of our investigation is *giant* galaxies, not dwarf ellipticals or “spheroidals.” As described in § 2, our photometric data and the analysis thereof are limited to galaxies not more than  $\sim 2$  mag fainter than present-day (unevolved)  $L^*$  at the redshift of each cluster examined. For objects with the typical colors of E+S0 galaxies, we are therefore discussing galaxies with  $M_B \lesssim -18.5$  (for our adopted cosmology).

Finally, the results reported here concern only cluster galaxies and do not necessarily bear on the evolution of field ellipticals. Moreover, because we use WFPC2 images that cover only the core regions of the distant clusters, we cannot address the evolution of galaxies located at larger clustercentric radii. Some studies of nearby clusters indicate that early-type galaxies located outside the core regions may have experienced recent star formation (Caldwell et al. 1993; Caldwell & Rose 1997). Almost all of these objects seem to be S0 galaxies.

## 2. OBSERVATIONS, REDUCTIONS, AND PHOTOMETRY

The overall sample of clusters for which we have collected photometric data is large and heterogeneous, consisting of 46 clusters (as of the time of this writing) at  $0 < z < 0.9$ , drawn from a variety of optical, X-ray, and radio-selected samples. In the present paper, we restrict our attention to a subsample of 19 clusters for which WFPC2 images were

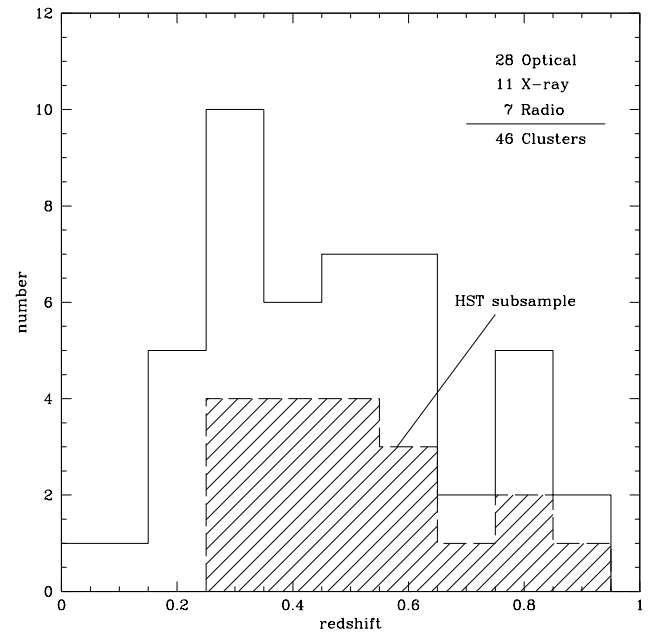


FIG. 1.—Redshift distribution of clusters in our complete imaging survey. Clusters with *HST* imaging, which are the subject of this paper, are shaded.

available to us. The redshift distributions of both the whole sample and the *HST* subsample are shown in Figure 1.

Optical and near-IR images of the clusters were obtained using CCD and HgCdTe array cameras on NOAO telescopes at Kitt Peak and Cerro Tololo in 1993–1996. This imaging provides multiwavelength photometric data of uniform quality through a standard set of filters, using well-understood photometric systems. These features are particularly advantageous when attempting to investigate systematically the evolution of large samples of faint gal-

TABLE 1  
CLUSTER SAMPLE

NAME	R. A. (J2000)	Decl. (J2000)	$z$	OBSERVED BANDS	$K_{\text{lim}}$ (mag)	$N_{\text{samp}}$		$N_{\text{pred}}$	
						Total	E/S0	Field	E/S0
AC 118 .....	00 14 19.30	−30 23 18	0.308	<i>gRJHK<sub>s</sub></i>	17.6	76	38	12	3
AC 103 .....	20 57 07.46	−64 38 53	0.311	<i>gRJHK<sub>s</sub></i>	17.6	72	32	12	3
MS 2137.3–234 .....	21 40 14.50	−23 39 41	0.313	<i>gRJHK<sub>s</sub></i>	17.6	34 <sup>a</sup>	21	12	3
Cl 2244–02 .....	22 47 12.90	−02 05 40	0.330	<i>gRJHK<sub>s</sub></i>	17.7	43 <sup>a</sup>	24	15	3
Abell 370 .....	02 39 53.81	−01 34 24	0.374	<i>RJHK</i>	17.9	79	52	18	4
Cl 0024+16 .....	00 26 35.42	+17 09 51	0.391	<i>gRJHK<sub>s</sub></i>	18.1	90	39	21	4
Abell 851 .....	09 43 02.60	+46 58 37	0.405	<i>RJHK</i>	18.2	71	33	23	4
GHO 0303+1706 .....	03 06 15.91	+17 19 17	0.418	<i>gRJHK<sub>s</sub></i>	18.3	80	38	25	5
3C295 .....	14 11 19.47	+52 12 21	0.461	<i>VIJHK<sub>s</sub></i>	18.5	63	25	28	5
F1557.19TC .....	04 12 51.65	−65 50 17	0.510	<i>VIJHK<sub>s</sub></i>	18.7	62	29	32	6
GHO 1601+4253 .....	16 03 10.55	+42 45 35	0.539	<i>VIJHK<sub>s</sub></i>	18.9	79	42	38	8
MS 0451.6–0306 .....	04 54 10.81	−03 00 57	0.539	<i>VIJHK<sub>s</sub></i>	18.9	101	51	38	8
Cl 0016+16 .....	00 18 33.64	+16 25 46	0.545	<i>VIJHK<sub>s</sub></i>	18.9	121	65	38	8
J1888.16CL .....	00 56 54.59	−27 40 31	0.560	<i>VIJHK<sub>s</sub></i>	19.0	70	38	40	10
3C 220.1 .....	09 32 39.61	+79 06 32	0.620	<i>VIJHK<sub>s</sub></i> <sup>b</sup>	19.2	59	22	49	12
3C 34 .....	01 10 18.53	+31 47 20	0.689	<i>VIJHK<sub>s</sub></i>	18.5 <sup>c</sup>	49	19	28	7
GHO 1322+3027 .....	13 24 49.29	+30 11 28	0.751	<i>RiJHK<sub>s</sub></i>	19.6	92	23	64	14
MS 1054.5–032 .....	10 56 59.53	−03 37 28	0.828	<i>RiJHK<sub>s</sub></i>	19.8	112	71	73	15
GHO 1603+4313 .....	16 04 18.89	+43 04 36	0.895	<i>RiJHK<sub>s</sub></i>	20.0	95	23	82	16

NOTE.—Units of right ascension are hours, minutes, and seconds, and units of declination are degrees, arcminutes, and arcseconds.

<sup>a</sup> WFPC2 image not centered on cluster.

<sup>b</sup> V/I photometry from WFPC2 F555W/F814W images.

<sup>c</sup> Limiting magnitude only  $K^* + 1$  owing to relatively shallow WFPC2 image.

axes over a broad redshift range. The sample of clusters studied here, along with the bandpasses used, is summarized in Table 1. In the near-infrared, atmospheric transmission windows require us to use fixed bandpasses, so we have imaged through standard  $J$ ,  $H$ , and  $K_s$  filters. Therefore, the infrared bands probe different rest-frame wavelengths for clusters at different redshifts.

The optical imaging was generally obtained in two bands that we have adjusted according to the cluster redshift in order to ensure that they span the  $\lambda_0 \sim 4000 \text{ \AA}$  region in the cluster rest frame. The clusters were divided into three redshift ranges for this purpose:  $0.3 < z < 0.45$  ( $g$  and  $R$  bands);  $0.45 < z < 0.7$  ( $V$  and  $I$  bands); and  $0.7 < z < 0.9$  ( $R$  and  $I$  bands). Our optical data set contains Gunn  $i$ -band images of two clusters (MS 1054.5–0321 and GH0 1322+3027), obtained at the Palomar 5.08 m telescope in 1995 February. Photometry for data taken in the Gunn-Thuan filters were transformed to the Landolt system using observations of spectrophotometric standards. Also, for 3C 220.1, we have used our WFPC2 F555W and F814W images to obtain  $VI$  photometry (after blurring the WFPC2 images to the seeing of our  $K$  image), using the calibrations given by Holtzman et al. (1995). For two clusters, Abell 370 and Abell 851, we do not have the desired  $g$ -band data. (Also it should be noted that the  $JHK$  data on A370 and A851 were obtained with PtSi detectors, as reported in SED95.) In this paper, we will generally refer to the two optical passbands as *blue* and *red*. The former measures rest-frame emission at wavelengths similar to or somewhat bluer than the rest-frame  $U$  band, while the latter corresponds to rest-frame wavelengths roughly from  $B$  to  $V$ .

Exposure times in all bandpasses were chosen to provide galaxy photometry with  $S/N > 5$  for galaxies with the spectral energy distributions of present-day ellipticals, down to  $\sim 2$  mag fainter than  $L^*$  (unevolved) at the cluster redshift. Table 1 lists the no-evolution  $K^* + 2$  mag ( $K_{\text{lim}}$ ) for each cluster. This permits us to study galaxy properties over a similar range of luminosities for all clusters in our sample, regardless of their redshift. The exact correspondence of the apparent magnitude range observed for a particular cluster to the luminosities of present-day galaxies depends both on  $q_0$  and on the degree of luminosity evolution in the galaxy population. Our images typically cover a field size of  $\sim 1$  Mpc at the cluster redshift, which is generally larger than that covered by the WFPC2 data used to select the early-type galaxy subsamples (see below). The optical data were calibrated onto the Landolt system wherein Vega has  $m_V = +0.03$ , and the IR images onto the CIT system wherein Vega has  $m = 0$ . The typical rms of the transformations is 0.02 in the optical and 0.03 in the near-IR. The effective angular resolution of the images is generally limited by the large pixel scale of the infrared arrays and is  $\sim 1''.7$  for the  $z < 0.6$  clusters and  $\sim 1''.2$  for the more distant objects.

Images in all bandpasses were co-aligned and convolved to matching point-spread functions (PSFs) in order to ensure uniform photometry at all wavelengths through fixed apertures. Object detection was carried out on the  $K$  images using a modified version (K. Adelberger 1996, private communication) of FOCAS (Valdes 1982), which was also used to obtain photometry in each band through circular apertures with a diameter equal to twice the PSF FWHM. The “ $N_{\text{samp}}(\text{total})$ ” column in Table 1 gives the total number of galaxies brighter than  $K_{\text{lim}}$  detected in the area of a WFPC2 field within our  $K$  images. In calcu-

lating  $K_{\text{lim}}$ , we have corrected for the tendency of FOCAS to measure “total” magnitudes that are somewhat fainter than the “true” total magnitude. So the  $K_{\text{lim}}$  listed in Table 1 are directly comparable to the photometry displayed in Figure 2 (see below). The observing methods, data reduction techniques, and photometric methods for our ground-based data set are described in detail in SED95. All photometry has been corrected for reddening using the interstellar extinction curve given in Mathis (1990), with values for  $E(B - V)$  taken from Burstein & Heiles (1982).

Morphological selection of E+S0 galaxies was done on the basis of *HST* WFPC2 images, except for Abell 370, for which preresubmission WF/PC data were used with galaxy classifications kindly provided to us by A. Oemler. The WFPC2 data were drawn from the *HST* archive, excepting MS 1054.5–032, for which the images were kindly provided by M. Donahue, and 3C 220.1, which is from our own imaging program (Dickinson & Broadhurst 1998). For each cluster, separate exposures reduced by the STScI pipeline procedure were brought into registration as necessary and were combined with iterative rejection to remove cosmic rays and pixel defects. The exposure times ranged from three orbits at the lowest redshifts up to 16 orbits on the most distant cluster. Morphological classification was performed independently by two of the authors on the summed WFPC2 images, which were usually in the F702W or F814W filters (using the reddest band where more than one was available). Objects were classified into the following groups: E/S0, Sa/b, Sc/d, Irr, disturbed/interacting galaxies, or stars. We do not attempt here to distinguish between E and S0 galaxies, so the analysis presented in this paper considers these galaxy types together as a single class. Comparison between the classifications of the two authors showed agreement (within the same group) for  $\sim 75\%$  of the objects. For the remaining  $\sim 25\%$ , nearly all of which had types differing by one group, a consensus was reached. Because the typing was done primarily for fairly bright galaxies (e.g., to  $I \sim 21.7$  for the  $z \sim 0.5$  clusters) and because it is used here only to distinguish early-type galaxies from all other types, misclassification is unlikely to be an important problem. The number of E+S0 galaxies brighter than  $K_{\text{lim}}$  identified in each cluster is given in the “ $N_{\text{samp}}(\text{E/S0})$ ” column in Table 1. In 3C 34, the available WFPC2 data were too shallow to allow morphological typing to reach the desired  $K$  magnitude limit; the typing was performed to only  $K^* + 1$  in this case.

### 3. EVOLUTION OF THE COLOR-MAGNITUDE SEQUENCE

We have chosen to characterize our results by focusing on the *average* properties of the early-type galaxies in each of the clusters, as represented by the intercept, slope, and scatter of the galaxy color-magnitude relation in four observed-frame colors: *blue*– $K$ , *red*– $K$ ,  $J$ – $K$ , and  $H$ – $K$ . Figure 2 shows these  $C$ - $M$  diagrams for 17 of the clusters in our *HST* subsample (those for A370 and A851 having been previously published in SED95). The early-type galaxies selected from the WFPC2 images are indicated by the solid circles. A tight color-magnitude sequence of the *HST*-selected E+S0 galaxies is readily visible in Figure 2, which demonstrates the broad similarity of their spectrophotometric properties to those of early-type galaxies in nearby clusters. Evolutionary effects are measured by referencing these color-magnitude relations to those observed in the low-redshift ( $z = 0.023$ ) Coma Cluster and transforming

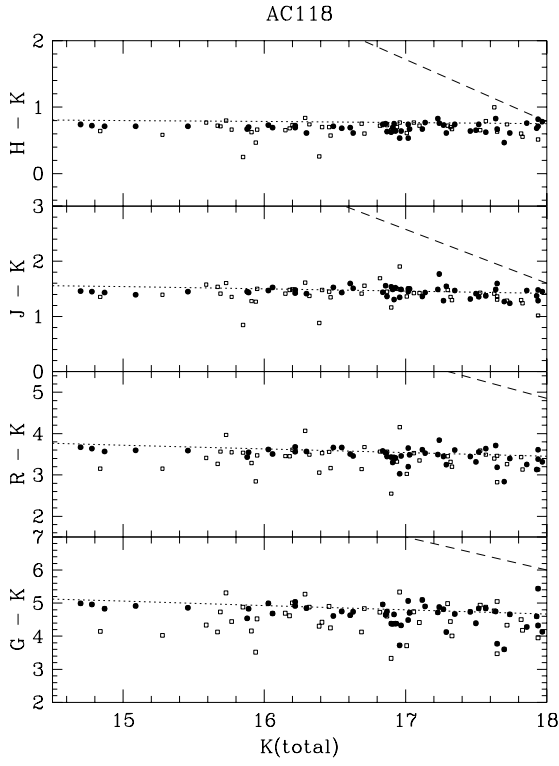


FIG. 2a

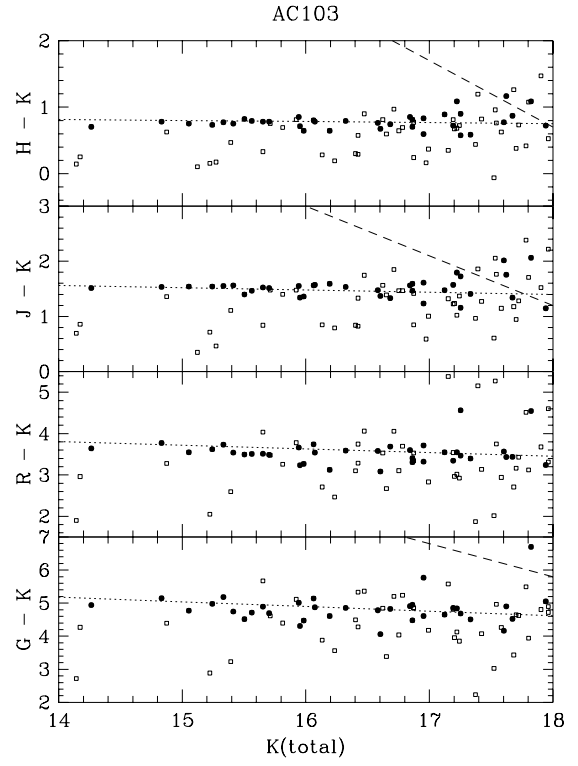


FIG. 2b

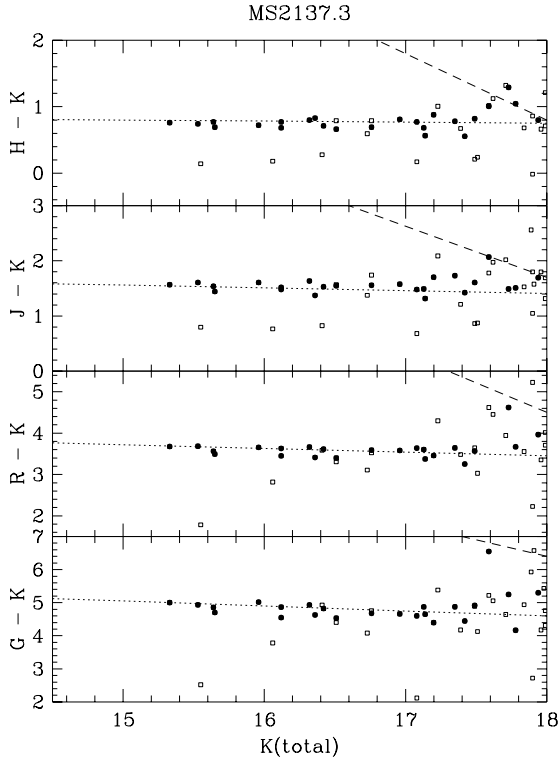


FIG. 2c

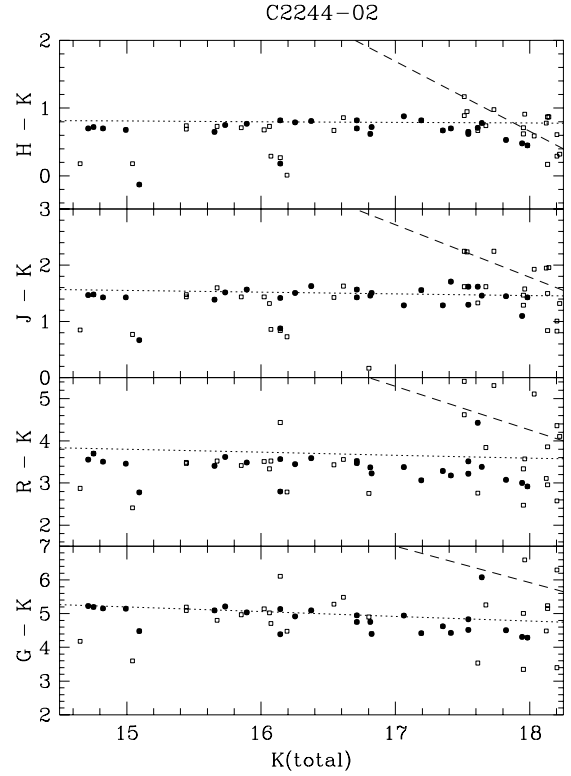


FIG. 2d

FIG. 2.—Color-magnitude diagrams for all of the clusters in the *HST* subsample, except for Abell 370 and Abell 851 (previously published in SED95). The clusters are arranged in redshift order, from low to high. The filled circles are the morphologically selected early-type galaxies in the WFPC2 field, and the open squares are all the other objects in the same area. Morphological identification was carried out for all objects in the WFPC2 field down to a limiting  $K$  magnitude of  $K^* + 2$  mag (except for 3C 34; see text for details). The slanting dashed lines mark the  $5\sigma$  limits in each color. The dotted lines show the color-magnitude relation for E+S0 galaxies in the Coma Cluster transformed out to the redshift of each cluster as described in the text; these represent the no-evolution loci.

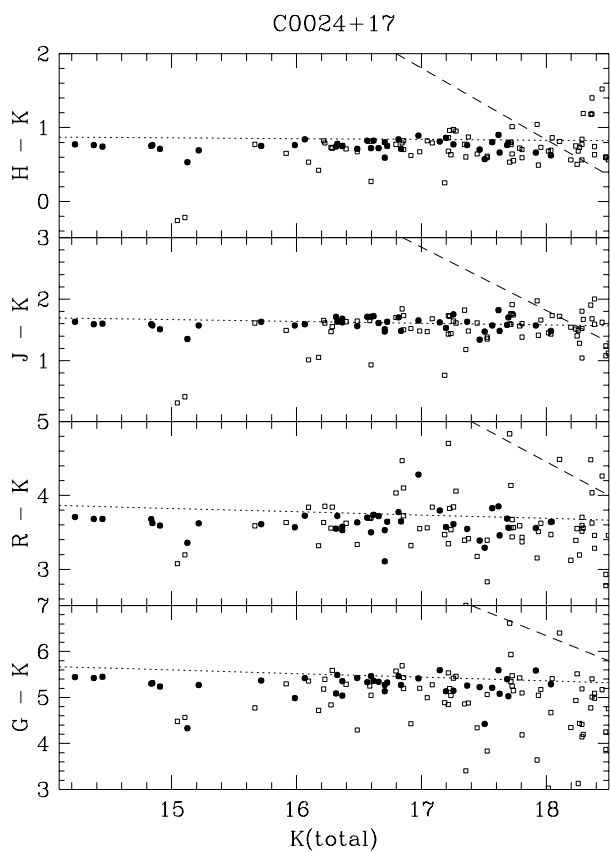


FIG. 2e

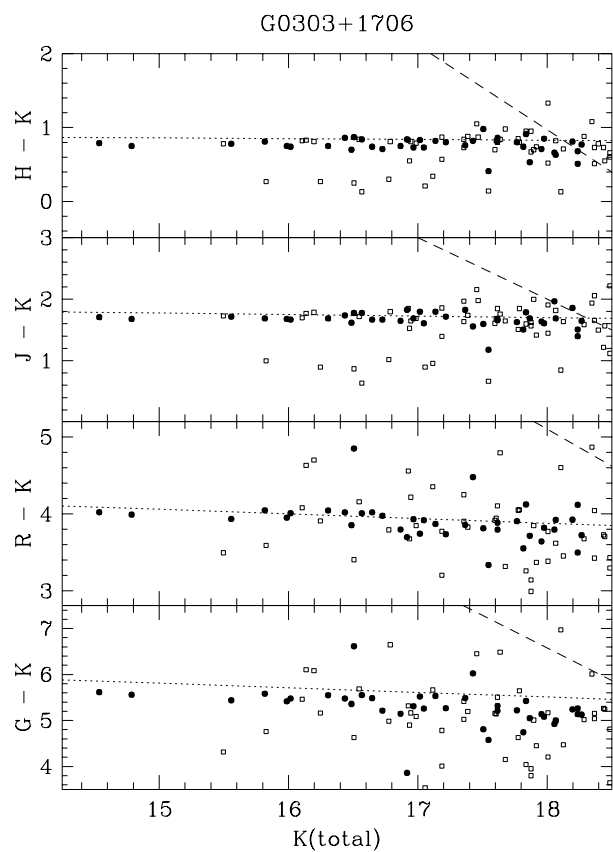


FIG. 2f

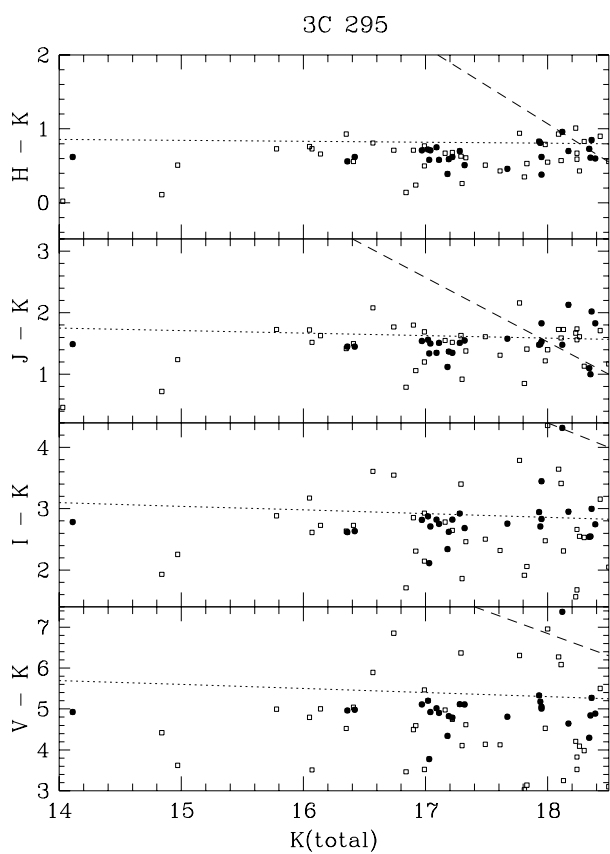


FIG. 2g

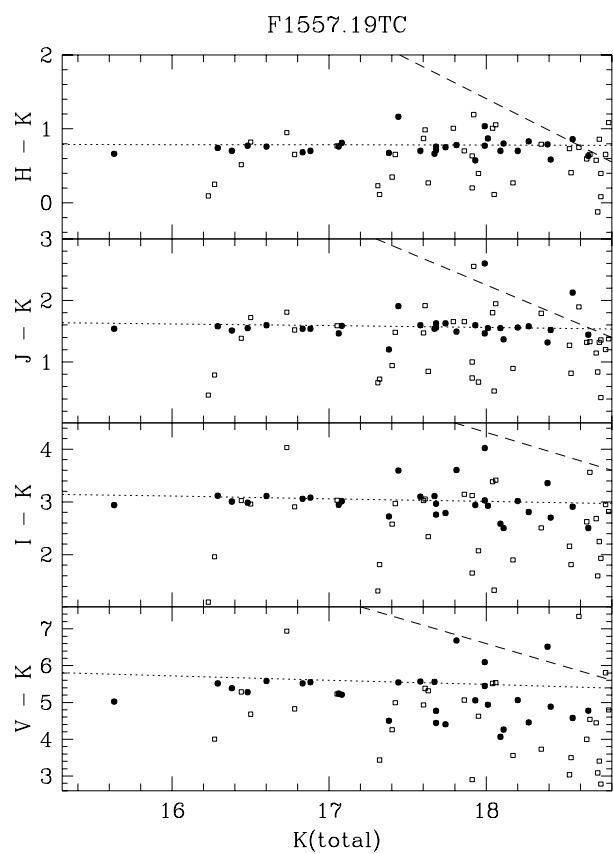


FIG. 2h

GH01601+4253

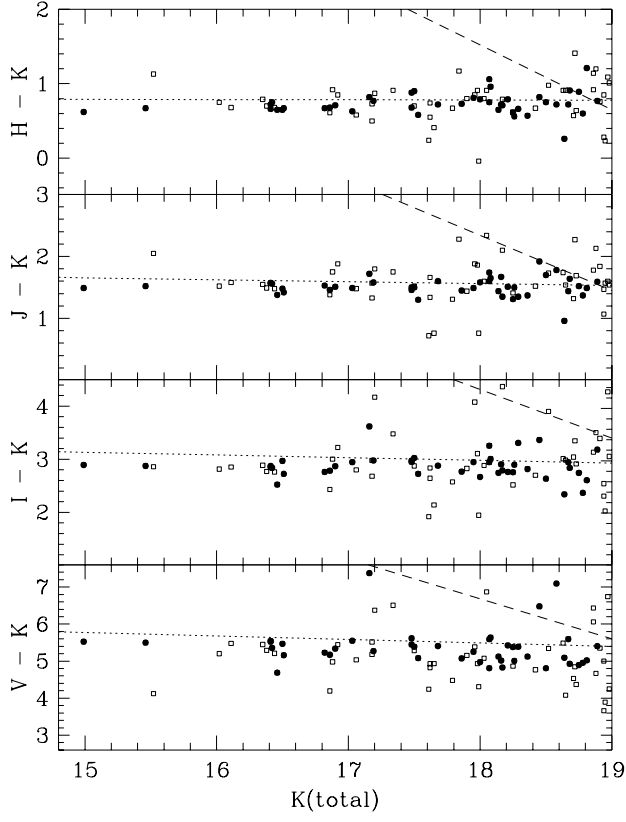


FIG. 2i

MS0451.6

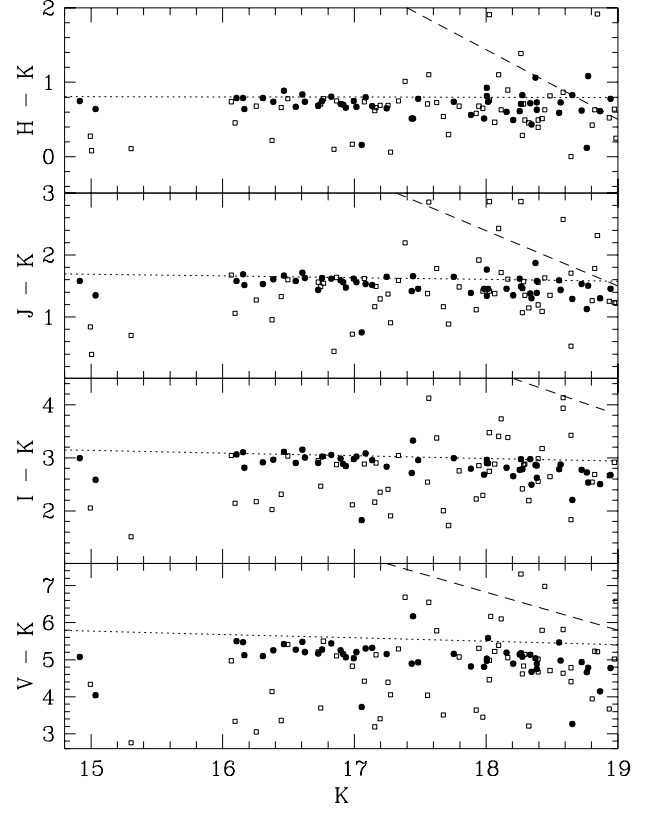


FIG. 2j

C0016+16

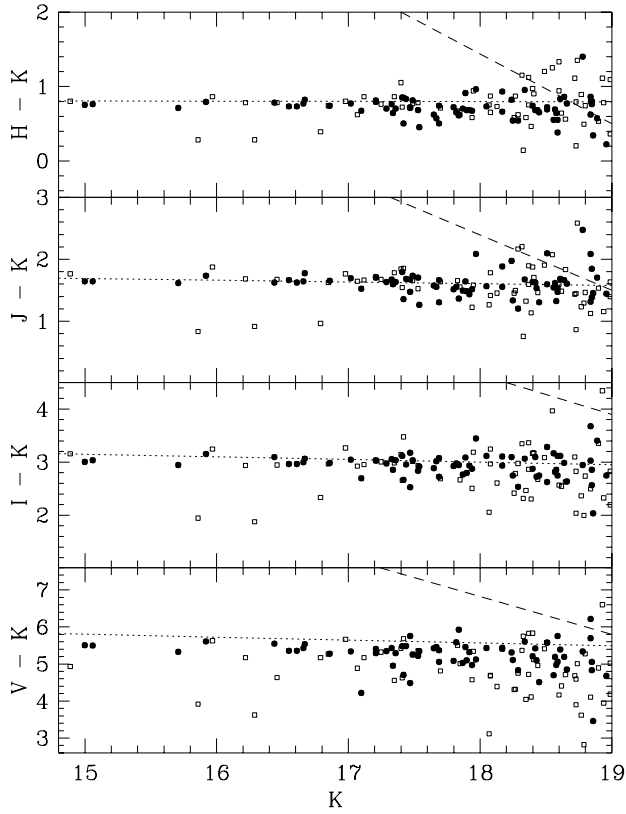


FIG. 2k

J1888.16CL

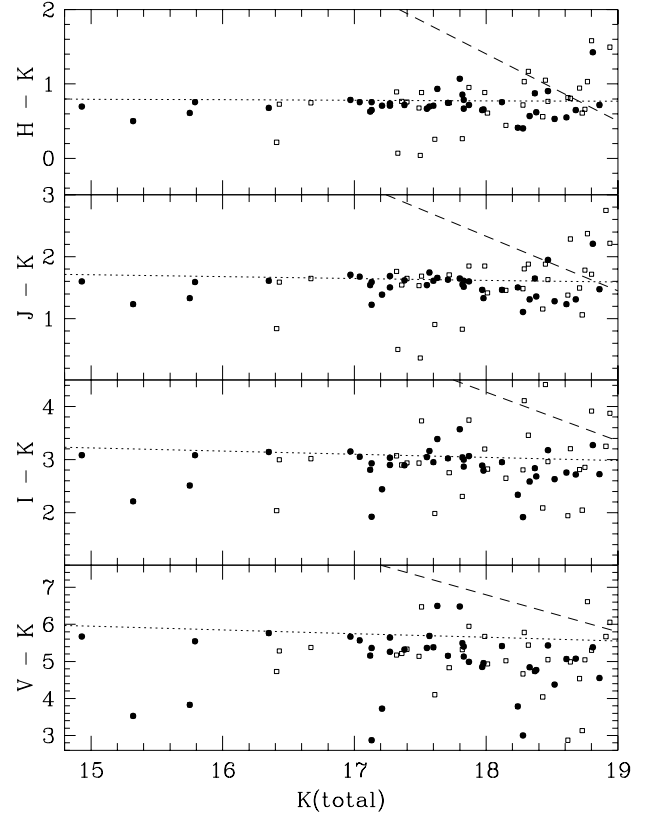


FIG. 2l

3C 220.1

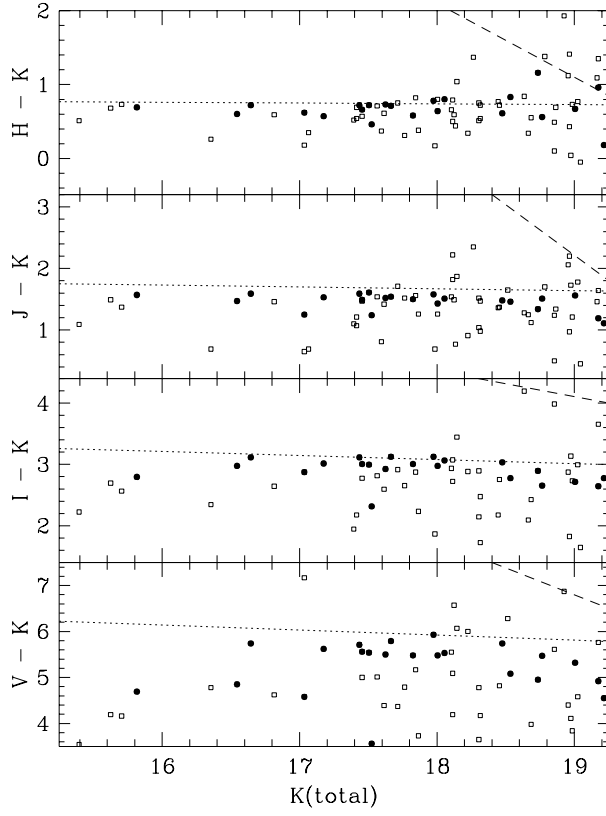


FIG. 2m

3C 34

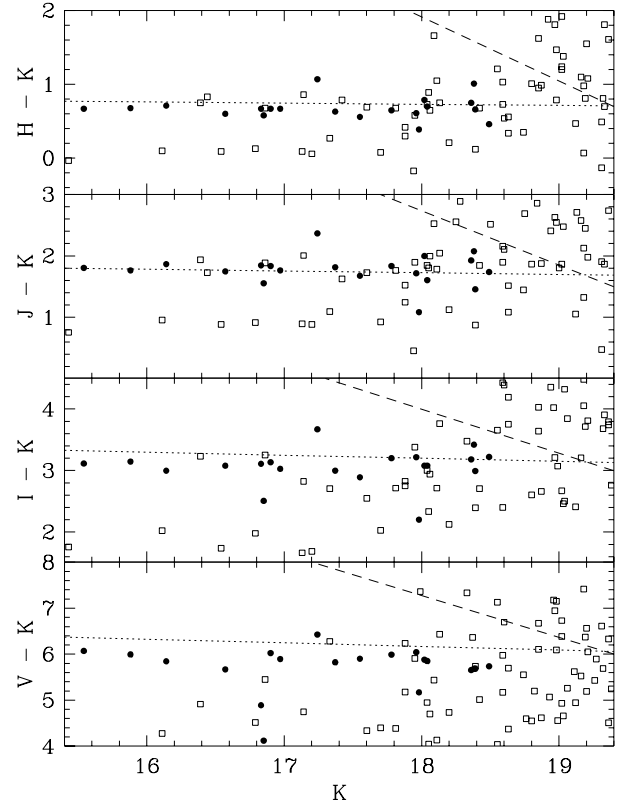


FIG. 2n

G1322+3027

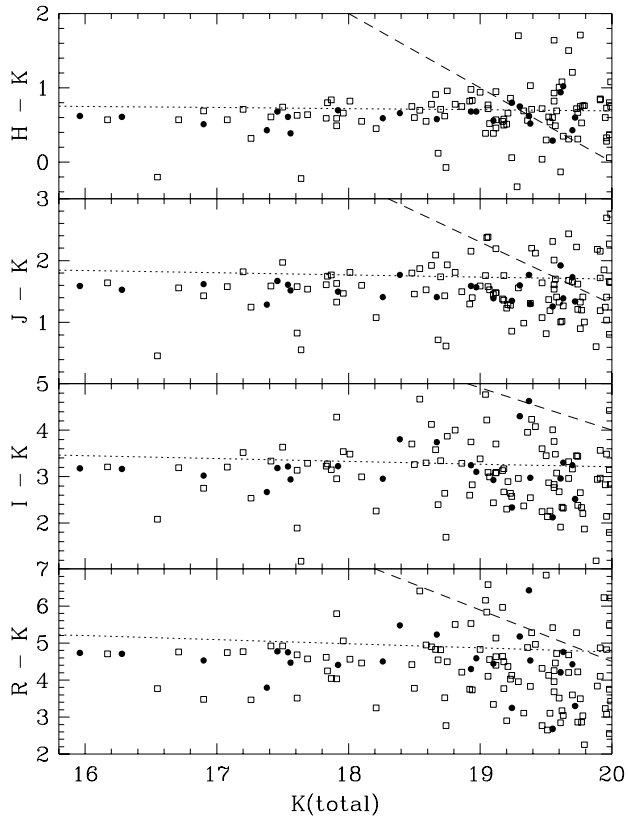


FIG. 2o

M1054.5-0321

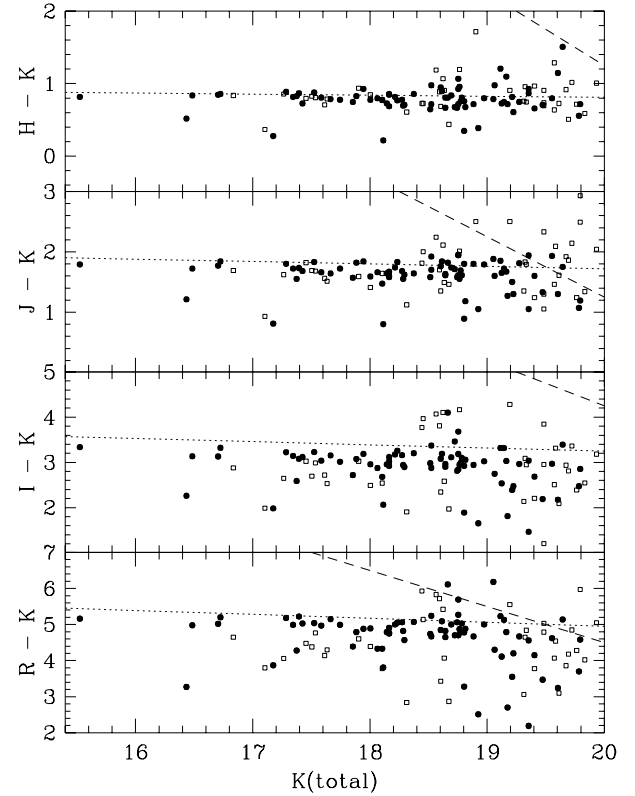


FIG. 2p



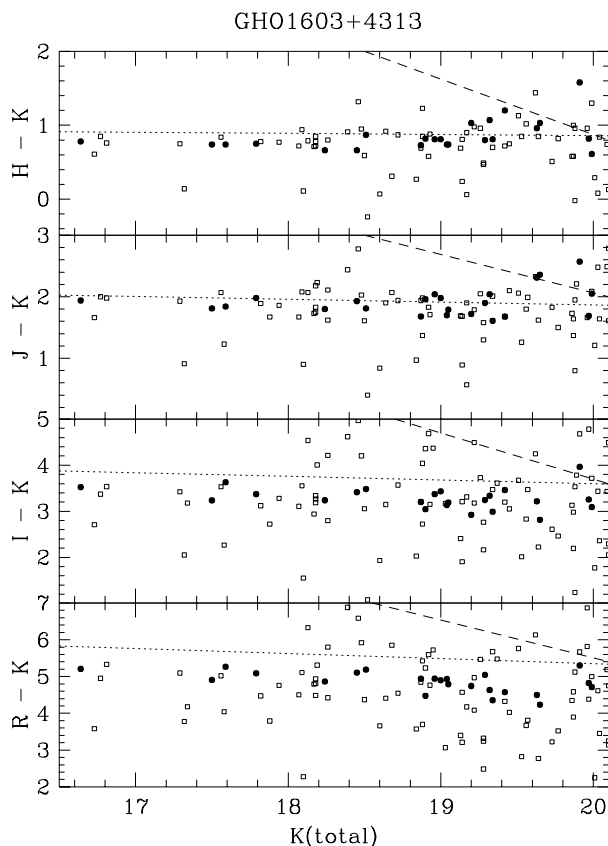


FIG. 2q

the latter to the high-redshift frame. The transformed Coma color-magnitude sequences in each color combination are represented by the dotted lines in each panel. These transformations are described in § 3.1. The intercept, slope, and scatter in the high redshift E + S0 color-magnitude relations are presented in §§ 3.2, 3.3, and 3.4 respectively.

### 3.1. Transformation of the Coma Color-Magnitude Relations

To the extent practical, we compare the photometry of distant E + S0 cluster galaxies to that of their low-redshift counterparts observed at similar rest-frame wavelengths. By making this comparison as directly as possible, we minimize the uncertainties in  $k$ -corrections and the dependence on spectral models. Our method follows that developed by, e.g., Lilly (1987) and Aragón-Salamanca et al. (1993) and is described in detail in SED95. We have obtained new images covering the central  $\sim 0.8$  Mpc of the Coma Cluster in the  $UBVRIZJHK_s$  bands down to  $\sim 5$  mag below  $L^*$  (Eisenhardt et al. 1998). The areal coverage of our Coma sample is similar to that of the distant clusters. This data set allows us to estimate the expected “no-evolution” colors in the observed bands for any distant cluster by interpolation among the observed bands on Coma. In other words, for each of our observed distant clusters, we determine the colors that E + S0 galaxies in Coma would appear to have if they were moved out to the relevant redshift and observed with the same filters used for the distant cluster.

To calculate the small  $k$ -corrections necessary for the interpolation, the spectrum of an 11 Gyr old model galaxy was constructed from the Bruzual & Charlot (1996; hereafter BC96) population synthesis code. The BC96 models are generated from libraries of model atmospheres for stars with various metallicities. Our template presumes a 1 Gyr

starburst followed by passive aging, a Salpeter IMF, and solar metallicity. This model provides an adequate fit to the average  $UBVRIZHK$  colors of the Coma early-type galaxies at  $\sim L^*$  and to a composite optical-IR spectrum (M. Rieke, private communication) made from observations of M32 and the M31 bulge. In the near-infrared, the agreement between the BC96 template and the Rieke spectrum is substantially improved compared to spectra generated using earlier versions of the Bruzual & Charlot code, particularly at  $\lambda \approx 1 \mu\text{m}$ . Because this template is used only for interpolation between adjacent bandpasses, the resulting uncertainties in the transformed Coma photometry should be small.

Finally, for each distant cluster, a linear fit was made to the transformed Coma photometry in color-magnitude space for each of the four observed-frame colors:  $blue-K$ ,  $red-K$ ,  $J-K$ , and  $H-K$ . These no-evolution color-magnitude relations are shown by the dotted lines in Figure 2.

### 3.2. Color Evolution

Color evolution in each of the 19 distant clusters was assessed by measuring the *differences* between the transformed Coma  $C-M$  relation and the colors of the early-type galaxies with  $K < K_{\text{lim}}$  selected from the WFPC2 images. The average color offset was determined in two ways. The biweight location estimator (Beers, Flynn, & Gebhardt 1990) was calculated using software kindly provided by T. Bird. A more traditional method was also tested in which an average (weighted by  $K$ -band flux) was calculated with one iteration of  $3\sigma$  clipping. In this procedure, the average and its dispersion are calculated, color differences greater than  $3\sigma$  from the average are removed, and then the average is calculated again. The main reason for employing the clipping is to reject galaxies that lie at redshifts different from the cluster. Because of the strong  $k$ -correction to the observed frame colors of distant ellipticals, foreground and background galaxies should appear to have substantially different colors from those of the main cluster locus. The biweight estimator is relatively stable against outliers. The two methods gave similar results for the average color differences.

Owing to the large number of early-type galaxies in most of the clusters, the random photometric errors in the average color differences computed here are small compared with the potential systematic errors. Combining in quadrature the uncertainties in the Coma photometric zero points, the distant cluster zero points, the extinction correction, PSF matching errors, color gradient corrections, and  $k$ -corrections, we estimate that the total systematic error is  $\sim 0.06$  mag in a color difference (see SED95 for a more thorough discussion).

The average color differences for the 19 clusters in the four observed colors are plotted against redshift in Figure 3, where the error bars are the uncertainties (*not* the scatter), including the estimated systematic errors. The horizontal dotted lines in Figure 3 at zero color difference represent no color evolution relative to Coma. A trend toward bluer rest-frame colors at higher redshifts is readily apparent in the  $blue-K$  and  $red-K$  data, and even to a small extent in the  $J-K$  data. The degree of color evolution is greater for the bluer rest-frame bands, as would be expected if more light from younger stars contributes to those bands at larger look-back times.

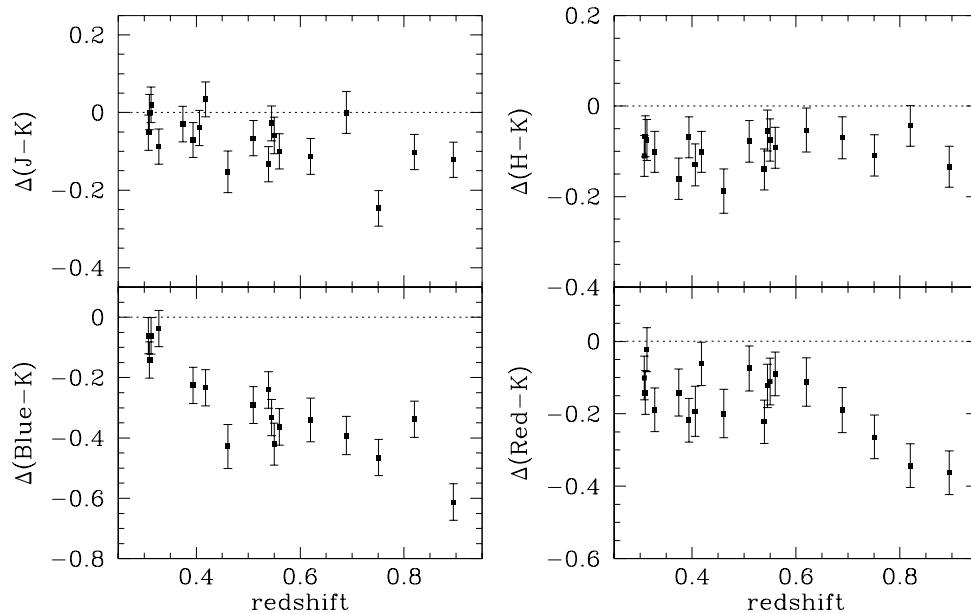


FIG. 3.—Color evolution in early-type galaxies in our distant cluster sample. The data points show average differences in the observed galaxy colors for each cluster relative to the same rest-frame colors of Coma E+S0 galaxies. A color difference of zero (indicated by the horizontal dotted lines) therefore represents no evolution relative to Coma. The error bars indicate the uncertainties in the averages, including our estimate of the systematic errors.

The reliability of the color trends seen in Figure 3 depends to a large extent on the question of cluster membership. Considering *all* of the galaxies within the  $K < K_{\text{lim}}$  samples, clearly many of the objects in the  $C-M$  diagrams of, e.g., GH0 1603+4313 in Figure 2*q* are not cluster members. While spectroscopic redshifts have been measured for some galaxies in this and other clusters, they are generally relatively few in number, and in many cases they remain unpublished. Field contamination of the early-type galaxy samples selected from within the WFPC2 fields, however, should be comparatively low. At both low and high redshifts, elliptical and S0 galaxies dominate the core regions of rich clusters (Oemler, Dressler, & Butcher 1997). Because the small WFPC2 fields primarily sample the cluster cores, the contrast of cluster E+S0 galaxies over the field population should be substantially enhanced relative to the overall galaxy sample. Therefore, we have elected *not* to correct for field galaxy contamination in a statistical sense.

The level of field galaxy pollution in a WFPC2 frame can be estimated by making use of published number counts and morphological fractions for the field galaxy population. In Table 1,  $N_{\text{pred}}(\text{field})$  gives the predicted number of field galaxies within the WFPC2 area down to  $K_{\text{lim}}$ , using the  $K$ -band number counts reported in Djorgovski et al. (1995).  $N_{\text{pred}}(\text{E/S0})$  is the expected number of field E+S0 galaxies, based on  $N_{\text{pred}}(\text{field})$  and the fraction of early-type galaxies as a function of “equivalent”  $\sim I$  magnitude given by Driver et al. (1995). The  $I$  magnitude used is that corresponding to the observed  $C-M$  relation at  $K_{\text{lim}}$ . (While it would be preferable to use morphological fractions as a function of  $K$  magnitude, such data are not yet available.) Clearly, the predicted field E/S0 contamination is uncertain, given the small volumes under consideration in each cluster and our inadequate knowledge of field galaxy morphological fractions at faint magnitudes. Taken at face value, the estimates suggest the early-type galaxy samples in most of our clusters are dominated by members, and hence the

modal properties of the entire E+S0 samples are representative of the properties of the true cluster galaxies. Figure 2 shows that the color trends we observe are characteristic of our sample and cannot be attributed to contaminating foreground galaxies. The relative fraction of early-type field galaxies may well be greater in the higher redshift clusters, but this is difficult to assess given the widely varying numbers seen in the clusters at  $z > 0.7$ . Nevertheless, nearly all of the early-type galaxies in the three highest redshift clusters are found to be bluer in  $R-K$  than the predicted no-evolution line, which indicates that the cluster members alone have bluer rest-frame colors than do cluster E+S0 galaxies today.

As a further check on contamination, statistical field corrections were applied to the complete  $C-M$  diagram data (without reference to galaxy morphology) in a manner similar to that described in SED95 but with a much larger and more homogeneous photometric data set on faint field galaxies (Elston, Eisenhardt, & Stanford 1998). Because of the strong effects of the  $k$ -corrections for early-type galaxies, the color distribution of field elliptical and S0 galaxies (which should span a wide range of redshifts) is expected to be broader than that of the cluster E+S0 galaxies, and in practice, several of the morphologically selected early-type galaxies with colors far from the no-evolution locus are removed by the statistical procedure. Average color differences of these field-corrected early-type samples for each cluster were calculated and found to be the same within the errors as those presented in Figure 3. It should be emphasized that the field corrections were applied only as a test of our results, which were calculated from the samples *without* field correction.

Other important issues bearing on the observed color evolution include zero-point errors and the transformation of the Coma colors. Even if the zero-point errors are as much as 0.1 mag (a factor of  $\sim 4$  higher than we believe to be the case), which would render the color differences at low redshift questionable, the higher redshift optical- $K$  color

differences would remain significant. As for the Coma-based no-evolution reference colors we calculate, the transformations should be accurate because they are based on *interpolations* within our own Coma photometry, which itself is in good agreement with published Coma data such as those of Bower et al. (1992) and Frogel et al. (1978).

### 3.3. Color-Magnitude Slopes

In all 19 of the clusters in our sample, a significant slope to the optical-IR color-magnitude relationship is evident among the early-type galaxies. As for present-day E+S0 galaxies (see, e.g., Sandage & Visvanathan 1978; De Propris et al. 1998), the slope of the relation is progressively steeper for colors measured at shorter wavelengths. We have fitted the slopes of the color-magnitude relation for each of our clusters in various bandpass combinations. For each cluster, the  $C-M$  fit was made to E+S0 galaxies brighter than  $K_{\text{lim}}$ , i.e., over the same range of absolute magnitudes relative to our assumed no-evolution value of  $K^*$ . Here it is important to restate that the optical-IR colors we are observing are *not* fixed in the cluster rest frame: the optical bands shift approximately with the cluster redshift, while the infrared bands remain fixed. Therefore, the wavelength baseline probed by, e.g., the *blue*– $K$  color becomes shorter toward higher redshifts because of the fixed  $K$  band. This, however, should have a relatively small effect on interpretation of the slopes measured here, since the intrinsic  $C-M$  slope for IR-IR colors is quite small. As a result, there is little difference in the slopes of the (e.g.) rest-frame  $U-J$  and  $U-K$  color-magnitude relations: the bulk of the slope in the color-magnitude relation comes from the blue rest frame stellar light.

In Figure 4 we plot the *difference* between the measured *blue*– $K$  versus  $K$  slopes and the slope of the Coma Cluster E+S0 galaxies at the same rest-frame wavelengths, evaluated from our transformed Coma photometry in the same fashion as described in § 3.1 above. A positive point in Figure 4 indicates that the cluster has a steeper slope than does Coma. The  $C-M$  slopes are consistent with those in Coma, suggesting that little or no *differential* color evolution (as a function of luminosity) has occurred in the early-type galaxy populations. Evidently, to the accuracy that we can measure, the color evolution of giant, early-type cluster

galaxies has been independent of luminosity, down to about 2 mag below  $L^*$ . We further discuss the implications below.

### 3.4. Scatter in the E+S0 Colors

As described in § 1, the small scatter observed for early-type galaxy colors around the mean locus of the color-magnitude relation has been used to argue that elliptical galaxies in the Coma and Virgo Clusters have had well-synchronized star formation histories (Bower et al. 1992). At higher redshifts, this test has been made by SED95 using rest-frame  $V-H$  colors in two clusters at  $z \approx 0.4$  and by Ellis et al. (1997) using rest-frame  $U-V$  colors in three clusters at  $z \approx 0.54$ . Here, we may apply the test to our sample of 19 clusters using a variety of color combinations over a broad interval of look-back time, from  $0 < z < 0.9$ . As described below, we restrict the sample to galaxies somewhat brighter than  $K_{\text{lim}}$  to measure the scatter more effectively.

Color scatters for the cluster E+S0 samples were calculated using the mean differences from the transformed Coma relation calculated in § 3.2 and plotted in Figure 3. The slope of the color-magnitude relation was assumed to be fixed at the Coma value for the appropriate bands, and the scatter about this mean relation was then computed. As is evident from Figure 4, the assumption of the Coma  $C-M$  slope is a reasonable one. Any error introduced by the assumption of an incorrect slope would tend to increase the scatter we measure relative to its true value. For each cluster, the observed color scatter and its uncertainty were calculated using the biweight scale estimator. The observed scatter includes contributions from both an *intrinsic* component of color scatter (real color variations among galaxies at a fixed luminosity) and from photometric uncertainty, which we will call the *measurement* scatter. In order to determine the level of the intrinsic component, we first estimate the measurement scatter and then subtract it in quadrature from the observed value. Measurement errors for individual galaxies are larger for fainter galaxies, and this must be taken into account when computing the overall measurement scatter expected for the cluster. Because less luminous galaxies are more numerous than bright ones, the overall measurement scatter tends to be dominated by the photometric errors associated with the fainter galaxies.

The photometric measurement uncertainty expected for each individual galaxy was determined using a calculated estimate of the signal-to-noise ratio based on the measured sky background noise and the galaxy photometry, in conjunction with simulations in which artificial galaxy images were added to the data at the appropriate magnitudes and colors and then measured with FOCAS. This procedure was described in SED95 and will be elaborated in Stanford et al. (1998). Next, a series of Monte Carlo simulations was carried out to estimate the total measurement error over a given magnitude range used in the estimate of the color-magnitude scatter. For each cluster, a list of galaxies was generated matching the actual  $K$  magnitudes of the observed E+S0 galaxies for that cluster. Colors were then assigned to each galaxy assuming *zero* intrinsic color variation plus random Gaussian noise appropriate to the magnitude of the galaxy. The artificial catalog was then run through the biweight estimator to compute its scatter. This process was repeated 1000 times for each cluster, and the results were averaged to provide a robust determination of the expected measurement scatter.

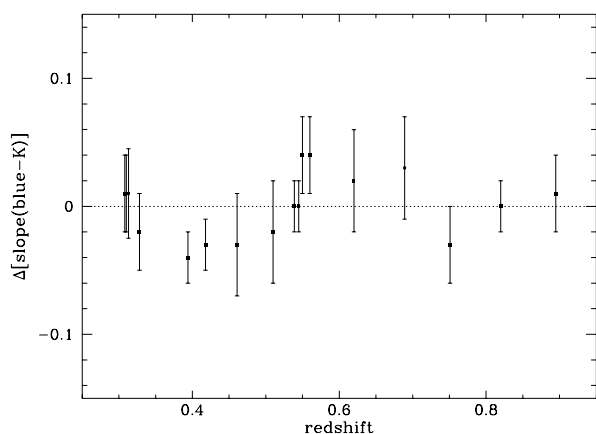


FIG. 4.—Difference between the fitted slopes of the *blue*– $K$  vs.  $K$  color-magnitude relation in each cluster and the corresponding slopes of the transformed Coma colors, as a function of redshift. The dotted horizontal line represents no evolution. The error bars are  $\pm 1 \sigma$  uncertainties.

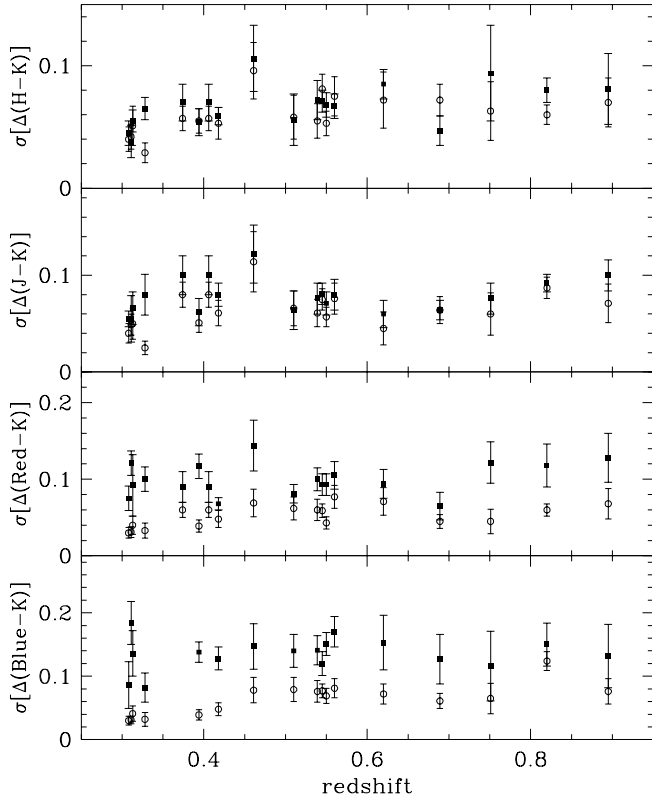


FIG. 5a

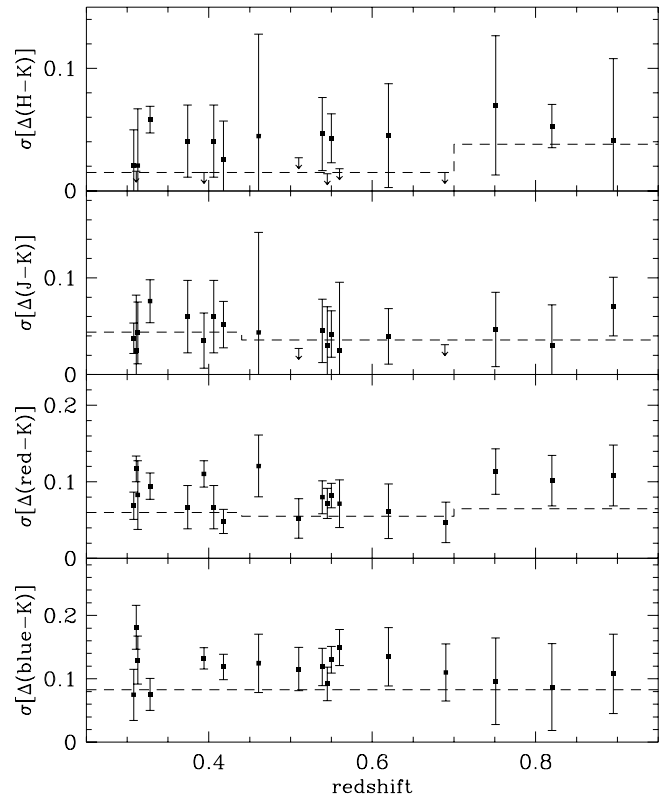


FIG. 5b

FIG. 5.—(a) The observed (filled squares) and measurement (open circles) scatter in the colors of early-type galaxies in our cluster samples. The error bars show  $\pm 1 \sigma$  uncertainties in the scatter values. (b) Intrinsic scatter in the galaxy colors for each cluster. The dashed lines represent the intrinsic scatter in similar rest frame colors for a sample of Coma E + S0 galaxies. The error bars are  $\pm 1 \sigma$  uncertainties in the scatter values.

Because, as noted above, photometric errors are larger for fainter galaxies, there is an optimal magnitude threshold down to which one should compute the  $C-M$  scatter. Using galaxies that are too faint inflates the measurement scatter. At the opposite extreme, using only a few bright galaxies leaves too few objects with which to determine the rms color variations, so that the biweight estimator provides only an uncertain determination of the observed scatter. The Monte Carlo simulations described above were repeated with various faint-end magnitude cutoffs to determine magnitude thresholds at which the cluster galaxy samples should be limited. For the low-redshift clusters ( $z < 0.5$ ), where the data generally reach somewhat deeper in the rest frame, this limit was set to  $K \leq K^* + 1$ . For clusters at  $0.5 < z < 0.7$ , it was set to  $K \leq K^* + 0.5$ , and for clusters at  $z > 0.7$ , the limit was set to  $K^*$ . The assumed value of  $K^*$  at each redshift assumes  $q_0 = 0.05$  and no luminosity evolution of the galaxy population. If allowance is made for either passive luminosity evolution or a larger value of  $q_0$ , the scatter calculations cover approximately the same range of luminosities at all redshifts. The varying sample depth would affect the estimated scatter only if the intrinsic scatter changes as a function of galaxy magnitude (see below).

The observed scatter and the estimates of the measurement scatter in the four colors spanning the observed wavelength range of our data are plotted for each cluster in Figure 5a. Using the subsample of early-type galaxies truncated to the appropriate  $K$  magnitude limit, the measurement scatter was then subtracted from the observed scatter in quadrature. The resulting estimates of the intrinsic rms

color scatter, together with their uncertainties, are plotted in Figure 5b. To facilitate comparison with similar results from optically based studies (e.g., Ellis et al. 1997), the intrinsic scatter in the purely optical *blue-red* color (very roughly  $U-V$  in the rest frame) is shown in Figure 6. For some clusters and bandpass combinations, only upper limits to the intrinsic scatter could be determined reliably. Note that implicit in our method of calculation is the assumption that the intrinsic color scatter in the cluster galaxies is independent of luminosity within a particular cluster. We do not test this here, but Bower et al. (1992)

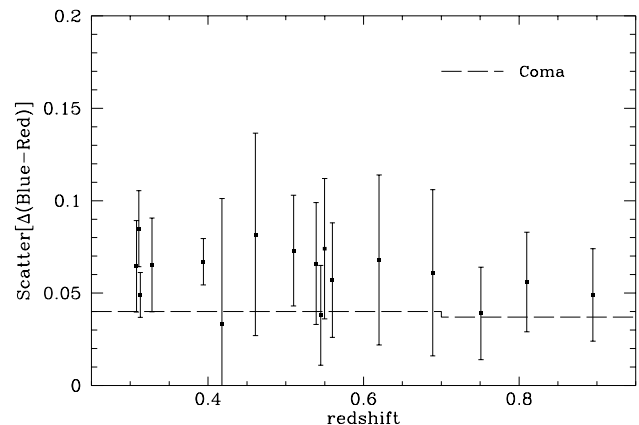


FIG. 6.—Intrinsic scatter in the purely optical *blue-red* colors of the early-type galaxies in each cluster with error bars representing  $\pm 1 \sigma$  uncertainties.

indicate that this is indeed the case for Coma and Virgo galaxies, while Ellis et al. (1997) suggest that it is true for rest-frame  $U-V$  colors of early-type galaxies in  $z \approx 0.5$  clusters as well.

The intrinsic color scatter shown in Figures 5 and 6 is remarkably constant with redshift in all colors. No significant trends toward increasing scatter at higher redshifts are observed. The dashed line in each panel shows the intrinsic scatter in a similar rest-frame color for the Coma E+S0 sample—our measurements of this scatter from the new Coma data are consistent with those reported by Bower et al. (1992). These color dispersions are independent of many of the uncertainties affecting the colors themselves, notably the photometric zero points, reddening corrections, seeing corrections, and color gradient corrections. To the extent that the lack of a field correction has caused non-cluster members to be included in the sample, the true scatter may be even lower than the calculated value. However, the constancy of the intrinsic scatter with redshift argues against field galaxy contamination being a significant effect.

#### 4. DISCUSSION

The overall picture that emerges from the data presented above is one of generally quiescent behavior for most early-type galaxies in clusters over at least half the age of the universe. The spectrophotometric evolution of the *majority* of relatively bright (and presumably massive) early-type galaxies in clusters over this time span appears to be smooth and steady. The parameters of the color-magnitude relation are very stable out to  $z \approx 0.9$ : while the intercept (i.e., the average E+S0 galaxy color at a particular luminosity) evolves gradually, both the slope and the scatter of galaxy colors around the mean relation change hardly at all.

By examining the evolution in the intercept, slope, and scatter of the galaxy color-magnitude relation, we are describing the *average* properties of early-type galaxies in rich clusters as a function of redshift. Therefore, the evidence that the evolution in these photometric properties has been “smooth and steady” does not exclude the possibility that *some* early-type cluster galaxies have followed different evolutionary trajectories, forming later or undergoing later episodes of star formation. Charlot & Silk (1994) and other authors have noted that a small amount of late star formation superimposed on an otherwise old elliptical galaxy leaves only a small imprint on its colors after approximately 1 Gyr. Therefore, individual galaxies in the clusters studied here may have experienced small, late episodes of star formation without standing out too far from the  $C-M$  locus. Indeed, if a few extremely blue (or red) ellipticals were present in the cluster, these would not strongly perturb the biweight scale estimator used to determine the color scatter.

It is also conceivable that the way in which we have constructed our sample has created a sort of “tunnel vision” that systematically excludes the actively evolving predecessors of early-type cluster galaxies in today’s universe. We conclude the discussion by considering the possible role of selection effects on our results.

##### 4.1. Color Evolution

The trends of the optical- $K$  colors with redshift presented in § 3.2 and Figure 3 clearly demonstrate that early-type galaxies in clusters have evolved since  $z \sim 1$ . They are in broad agreement with similar results from Dressler & Gunn (1990), Aragón-Salamanca et al. (1993), Rakos & Schombert

(1995), and Lubin (1996). Such a bluing trend is expected from passive evolution of a stellar population. As one approaches younger ages at higher redshifts, the color of the main-sequence turnoff for the bulk of the stellar population becomes bluer. The IR-IR colors show little change with redshift, as expected since the near-infrared light from early-type galaxies is dominated by giant stars with little contribution from the main sequence turnoff population. At the higher redshifts, however, even the  $J-K$  colors have become bluer, in part because the observed  $J$ -band samples the rest-frame  $R$  band by  $z \approx 0.9$ .

Some comparison of the observed evolution with models is instructive, if not definitive. If early-type cluster galaxies were genuinely a uniform population of well-synchronized galaxies evolving in a purely passive fashion, then it would in principle be possible (with sufficiently accurate data) to compare their spectrophotometric properties to predictions from reliable population synthesis models, so as to jointly constrain the evolutionary histories (e.g., formation redshift and star formation timescale) and perhaps the cosmological parameters (which set the relation between redshift and time). In practice, at this stage it is unwise to push such comparisons too far: the data have their limitations, and so do existing models (see Charlot, Worthey, & Bressan 1996). Moreover, the number of adjustable parameters is large. Here we choose to use the models simply to demonstrate the expected behavior from broad classes of star formation histories, rather than attempt to uniquely specify acceptable models from our data.

In Figure 7, we repeat the E+S0 color measurements from Figure 3, extending the redshift axis to  $z = 0$  to include Coma, which lies at zero color difference by definition. In each panel of Figure 7, we show several tracks representing predictions for color evolution from the spectral synthesis models of Bruzual & Charlot (1996). As with the data, the model curves represent color *differences* relative to present-day Coma galaxies and were calculated in the same way as were the color differences of the data. (The occasional sharp inflections in the model color tracks, e.g., for  $blue-K$  at  $z = 0.7$ , reflect the changes with  $z$  in the filter bandpasses used for the optical data.) In the models, the star formation occurs in a 1 Gyr burst governed by a Salpeter IMF and evolves passively thereafter. For one of the cosmologies, we have computed models for two formation redshifts,  $z_f = 2$  and 5, where “formation” is defined as the redshift at which star formation begins. For our adopted cosmology of  $q_0 = 0.05$  and  $H_0 = 65 \text{ km s}^{-1} \text{ Mpc}^{-1}$ , star formation in these two models ceased at  $z = 1.5$  and 3.1, and the resulting present-day ( $z = 0$ ) galaxy ages would be 9.7 and 11.9 Gyr, respectively. We may broadly consider the two models with differing  $z_f$  to represent “late” and “early” formation epochs for the bulk of the stars in early-type cluster galaxies.

For the optical-IR colors, particularly the  $blue-K$  data, the “late” formation models are substantially bluer than the observed galaxy colors at  $z > 0.6$ . For these particular population synthesis models, this corresponds to a limit on the mean ages of early-type galaxies in high-redshift clusters: model ages younger than  $\sim 4$  Gyr at  $z = 0.6$  or  $\sim 2.7$  Gyr at  $z = 0.9$  produce colors too blue to match the actual cluster galaxies. Also plotted in Figure 7 are two other BC96 models in which the formation redshift is fixed at  $z_f = 5$  and the cosmology (and hence galaxy age at a given redshift) is allowed to vary. There is no strong preference for

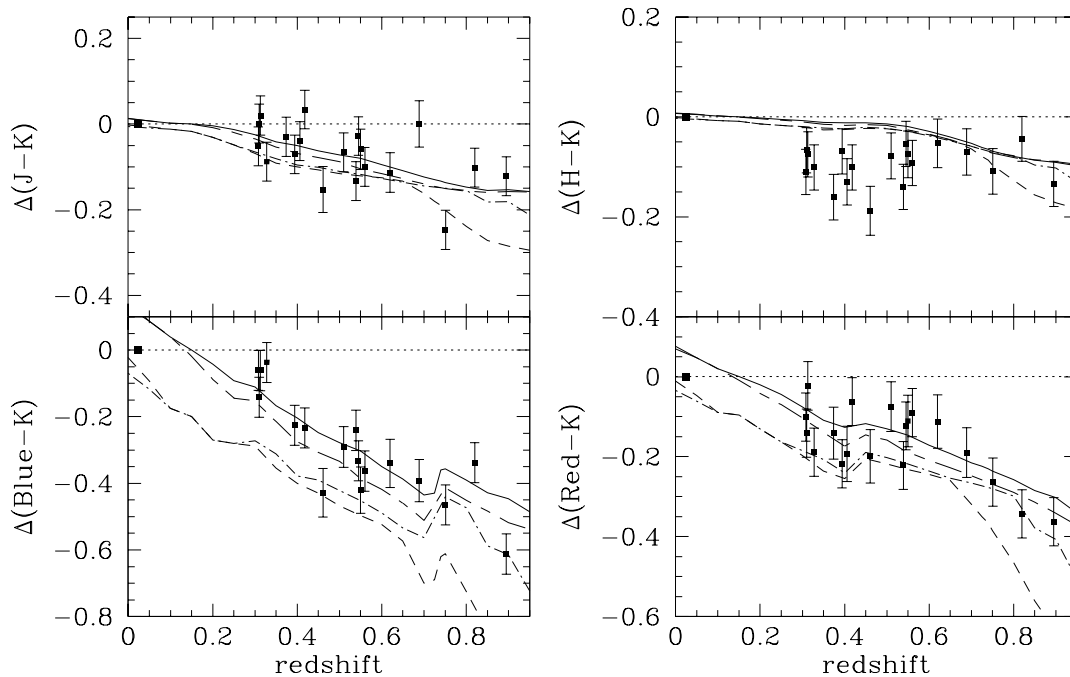


FIG. 7.—Color evolution in distant cluster E+S0 galaxies, as presented in Fig. 3 but with the redshift axis extended to  $z = 0$  to include Coma, which by definition falls at zero color difference and is represented by the points with no error bars. In each panel, four Bruzual & Charlot (1996) evolutionary synthesis models are plotted. Each line follows the evolution of a 1 Gyr burst of star formation with solar metallicity, plotted with the following variations:  $z_f = 5$ ,  $h = 0.65$ , and  $q_0 = 0.05$  (solid line);  $z_f = 2$ ,  $h = 0.65$ , and  $q_0 = 0.05$  (short-dashed line);  $z_f = 5$ ,  $h = 0.5$ , and  $q_0 = 0.5$  (short-dashed-long-dashed line);  $z_f = 5$ ,  $h = 0.8$ , and  $q_0 = 0.1$  (dot-dashed line). The inflection in the *blue*–*K* model colors at  $z \approx 0.7$  is due to the change of filters used for the observations from the *V* to *R* band at this redshift.

one of the cosmologies with the higher  $z_f$  shown in Figure 7 if allowance is made for small zero-point shifts in the model tracks.

One curious discrepancy for all clusters occurs in the *H*–*K* colors. At all redshifts, the clusters are systematically bluer than the no-evolution Coma expectation by approximately 0.1 mag. The same effect was noted for two clusters at  $z \approx 0.4$  in SED95. The population synthesis models predict very little evolution in this color out to  $z \approx 0.6$ , so the effect is difficult to understand. In the rest frame, the *H* band passes from  $\sim 1.25$  to  $\sim 1 \mu\text{m}$  in this redshift range—a part of the spectral energy distribution of present-epoch galaxies known poorly at best. Therefore the observed *H*–*K* color at  $z \leq 0.6$  is sliding through one of the most uncertain spectral regions of spectral synthesis models. However, it is important to recall that the  $\Delta(H-K)$  measurements presented for the data are *not* made with respect to the models, but relative to photometry of real galaxies in the Coma Cluster. Systematic zero-point errors in the high-redshift cluster data seem unlikely, since the data were collected during many different observing runs with several instruments on several telescopes. The infrared Coma photometry we have used to make the comparison is in good agreement with other published data sets. Although real evolution at rest frame  $\sim 1.1 \mu\text{m}$  over look-back times of order 3–5 Gyr seems improbable, we have no other explanation for the (admittedly small) effect.

There are no dramatic “outlier” clusters in our sample for which the *average* properties of their early-type galaxies (colors, scatter, or *C*–*M* slope) are drastically different from those of other clusters at similar redshift. This is particularly important given that the clusters studied here span a broad range of richness and X-ray luminosity. Recall that there is

no selection criterion for our sample other than that a cluster has WFPC2 imaging available. Most of these clusters, therefore, are rich and famous, accounting for their inclusion in *HST* imaging programs, but several (particularly the radio-selected clusters 3C 295, 3C 220.1, and 3C 34) are relatively poor in early-type galaxies. X-ray measurements, which are available for most of the clusters, show a wide range in luminosity, from  $3.0 \times 10^{43} \text{ ergs s}^{-1}$  for F1557.19TC to  $2.0 \times 10^{45} \text{ ergs s}^{-1}$  for MS 0451.6–036 (P. Rosati, private communication). The widely differing optical richnesses of these two clusters, both of which are at  $z \sim 0.5$ , correspond to their substantially different X-ray luminosities. The average colors of the early-type populations in these two clusters are nearly the same, and the same is true for the color scatter. These similarities indicate that E+S0 galaxy evolution is independent of cluster richness, as well as the degree of central concentration. The foregoing suggests that early-type galaxy evolution does not depend strongly on environment, at least above a certain minimum density threshold corresponding to poor clusters.

#### 4.2. Color-Magnitude Relationship

We find no evidence for a systematic change of slope in the color-magnitude relation of early-type cluster galaxies out to  $z = 0.9$ . Color evolution is thus essentially independent of luminosity for cluster early-type galaxies brighter than  $\sim 2 \text{ mag}$  below  $L^*$ . This strongly suggests that the slope in the color-magnitude relation is fundamentally a consequence of metallicity effects and not one of age, since less massive cluster E+S0 galaxies show no sign of being younger than their brighter, more massive counterparts. There is also no indication of differential chemical evolution over the look-back time of our sample, which could also

result in a change of slope. The observed behavior is as expected if the bulk of star formation in early-type cluster galaxies ceased long before  $z = 0.9$  and the galaxies remained largely fixed in their original mass-metallicity sequence—i.e., without substantial later merging to reshuffle the metallicity distributions.

Following the ELS formation scenario, models by Kodama & Arimoto (1997) predict little evolution in the color-magnitude slope out to  $z = 1$  if its origin is due to metallicity in stellar populations formed at early epochs. However, when those authors match the present-day color-magnitude slope in clusters with a mass-dependent age variation among the early-type galaxies, they predict drastic changes in the slope for  $0 < z < 0.9$ , which we do not observe. In the recent models of Kauffmann & Charlot (1997), which investigate elliptical galaxy evolution in the context of hierarchical galaxy formation with chemical enrichment, the  $C-M$  relation is established and preserved despite extensive merging because more massive and metal-rich ellipticals are formed by mergers of more massive and metal-rich spiral progenitors. In these models, there is a progressive flattening of the color-magnitude sequence with increasing redshift. However, the change in the slope is not dramatic until  $z > 1$ .

#### 4.3. Intrinsic Color Scatter and Early-Type Galaxy Formation

A small scatter in the colors of galaxies at a given luminosity implies that their stellar populations are similar. In particular, as noted previously, various authors (e.g., Bower et al. 1992) have used the small scatter of  $E+S0$  colors in nearby clusters to argue that the *fractional* differences in ages between the stellar populations of the galaxies are small, which sets a joint constraint on their ages and relative star formation histories. Either the early-type galaxies in Coma formed so long ago that color differences resulting from age variations have mostly damped out, or else their intrinsic age differences are very small. If  $E+S0$  galaxies in clusters share similar (but not identical) star formation histories, then we would expect the scatter in their colors to increase as one looks to higher redshifts, i.e., closer to the time when their last major episodes of star formation took place.

The degree to which the intrinsic color scatter of luminous early-type galaxies in clusters remains approximately constant over the very broad look-back time interval of our sample is perhaps the most striking result of this study. There is no evidence for a monotonic trend in the amplitude of the scatter over the redshift range  $0.3 < z < 0.9$  in any of the color combinations we have examined. The *blue*–*K* and *red*–*K* color scatter in the early-type galaxies for most of the distant clusters do appear to be systematically larger than is measured in samples of similar galaxies in the Coma cluster. While we believe that it may well be real, the difference is small. The smaller color scatter among Coma galaxies may represent a real “settling down” of the stellar populations in early-type cluster galaxies over the past few billion years since  $z = 0.3$ , but evidently the scatter was roughly constant over a period of several Gyr prior to that time. For our adopted  $q_0 = 0.05$  cosmology, the interval of look-back time from  $z = 0$  to  $0.3$  is nearly the same as that between  $z = 0.3$  and  $0.9$ , the redshift range of our cluster sample; it is slightly longer for  $q_0 = 0.5$ . Examining the scatter in the colors of  $E+S0$  galaxies in clusters at

$0.1 < z < 0.3$  should provide an interesting means of studying any transition which may have taken place during the last few billion years of cluster evolution.

If the intrinsic color scatter of early-type galaxies in present-day clusters were due to small age differences among otherwise passively evolving galaxies, then one would inevitably expect the scatter to have been larger at earlier times when the galaxies were younger and their *relative* age differences were greater. Similarly, if color variation among ellipticals reflects differences in their past merging histories, then we might expect to see increased scatter as we look back toward the era when the bulk of this merger activity took place. In either case, the resulting color variations will be damped as the time since the epoch of star formation lengthens, and the scatter in colors around the  $C-M$  relation should diminish toward  $z = 0$ . The fact that we do not see such trends over the redshift interval  $0.3 < z < 0.9$  suggests two possibilities. One is that the last episodes of major star formation in early-type galaxies took place several billion years before the look-back times at which we are observing the clusters, i.e., at redshifts significantly above one. In this case the color variations would have time to damp out, leaving a small and roughly constant value for the observed scatter. Alternatively, some other effect may act to erase the expected trend of scatter with redshift predicted from a uniform population. For example, some portion of the color scatter in early-type cluster galaxies could be due to metallicity variations at a fixed galaxy mass, i.e., a scatter in metallicities around the mean trend of the color-magnitude relation. This would then set a “floor” to the allowable scatter, which could act to reduce or erase some of the expected trend with age. It seems highly plausible that this should be the case, and such scenarios deserve further investigation, particularly as multimetallicity population synthesis models become more sophisticated. The models of Kauffmann & Charlot (1997) produce cluster ellipticals of a given mass exhibiting a range of metallicities that partially accounts for the scatter in their colors. If, however, the intrinsic scatter is partially a metallicity effect, then the argument for highly synchronized star formation histories remains valid and is perhaps strengthened: the component of scatter due to age variations must be even smaller than for models without metallicity variations, which requires a strong degree of uniformity in the ages of the stellar populations.

Another possibility is that the color scatter at any redshift has some component due to more recent episodes of star formation involving the early-type cluster galaxies. In this case, the assumption of purely passive evolution and thus strict coevality would be incorrect. The resulting effect on the galaxy colors and their scatter would then depend on the rate at which new star formation occurs. If the addition of young stars to cluster  $E+S0$  galaxies (e.g., during merger events) were small, stochastic, and more or less constant with redshift, then it could introduce a similar amount of scatter into the color-magnitude relation over the redshift range we are observing. To some degree, this interpretation may be related to the Butcher-Oemler effect in the context of the scenario advocated by Couch & Sharples (1987; hereafter CS87) and more recently developed by Barger et al. (1997). In these papers, the Butcher-Oemler effect is described as a starburst phase through which nearly *all* cluster galaxies pass at some point in their lifetimes. Evidence in favor of such a scenario includes the red  $H\delta$ -strong

galaxies of CS87 and the E + A galaxies of Dressler & Gunn (1983), though the latter may no longer be supportive given that WFPC2 imaging has shown that the E + A galaxies are generally disks (Wirth, Koo, & Kron 1994; Belloni et al. 1998). In the CS87 scenario, small amounts of recent star formation in the early-type galaxies, which might go undetected in terms of the effect on the average colors seen in Figure 3, would show up as increased color scatter. However, the monotonic color evolution trend with redshift seen in Figure 3 argues that such events are relatively unimportant to the overall stellar population.

The small scatter found in the early-type galaxy colors at the highest redshift in our sample places the most stringent constraint on the formation redshift and/or the coevality of the early-type galaxy populations. Following Bower et al. (1992), a simple comparison of the rate of change in the colors of a single-burst stellar population (BC96) model to the estimated intrinsic scatter yields a lower limit to the galaxy age at the cluster redshift. The intrinsic scatter in the observed frame colors *blue* – *K* and *red* – *K* of the early-type galaxies in GH0 1603 + 4313 is  $0.11 \pm 0.06$  and  $0.10 \pm 0.04$ , respectively. If early-type galaxy formation within this cluster occurred at times distributed uniformly across the collapse epoch (i.e., the  $\beta = 1$  case of Bower et al.), then the mean galaxy age at  $z = 0.895$  must be at least 3.9 Gyr. The resulting limit to the formation redshift is  $z \geq 3.0^{+0.0}_{-0.3}$ . This limit is consistent with the acceptable BC96 models for color evolution described in § 4.1. If galaxy formation occurred later, then the degree of synchronization must have been correspondingly greater: ages of  $\sim 2$  Gyr are admissible if galaxy formation were synchronized within a time interval of 500 million years. Again following the lead of Bower et al., the method described above can be turned around to estimate the amount of recent star formation. Assuming a fundamentally “old,” passively evolving model for early-type galaxy evolution, the intrinsic color scatter in GH0 1603 + 4313 limits small (e.g.,  $\leq 10\%$  by mass) bursts to have occurred at least 2 Gyr prior to its cosmic age at  $z = 0.9$ .

To summarize, the simplest interpretation of the scatter trends is that the stellar populations in most cluster early-type galaxies have been quiescent since at least  $z \approx 1.5$ . This ensemble behavior does not exclude the possibility that *some* cluster elliptical or S0 galaxies may have experienced star formation since that time. However, the striking similarity between the *C*–*M* relations for early-type galaxies in clusters at redshifts as large as 0.9 (e.g., Fig. 2) and those in Coma today certainly suggests a strong degree of evolutionary continuity. Altogether, it remains to be seen whether realistic cluster and cluster galaxy evolution models can be constructed that match both the Butcher-Oemler effect in disk galaxies and the flat behavior of the color scatter versus redshift for early-type galaxies.

#### 4.4. Selection Effects

While the quiescent photometric behavior of early-type galaxies in our cluster sample strongly suggests a quiescent evolutionary history out to  $z \approx 1$ , it is important to consider the potential role of the sample selection criteria in predetermining such behavior. There are three primary selection criteria for galaxies in our sample: location in the cores of rich clusters; E or S0 morphology; and luminosity in the observed *K* band. As noted in § 1, selection by rest-frame near-IR luminosity should yield a mix of galaxy types

that does not strongly depend on redshift, which alleviates the bias toward UV-bright galaxies at higher redshift. Therefore, while one would expect more quiescent behavior in a *K*-selected sample than in an optically selected sample, *K*-selected samples provide a truer picture of intrinsic changes with redshift. However, the other selection criteria may be less benign.

Morphological galaxy selection may introduce a type of bias. Within each cluster, WFPC2 imaging has provided a sample of galaxies recognizable as morphological early-type galaxies. However, if an elliptical or S0 galaxy were undergoing an interaction or were forming during a major merger event, it might not be classified as an “early type” and thus could be excluded from our sample. By the time the merger morphology has settled down sufficiently for the galaxy to be classified as a normal E or S0 (i.e., when tidal tails, star-forming knots, multiple nuclei, remnant spiral arms, etc. have fully merged or faded away), much of the blue light from recent star formation may also have subsided, leaving only the dominant old stellar light. In this way, sample definition might partially account for the small scatter in galaxy colors that we observe. If the antecedents of some of today’s early-type galaxies cannot be recognized by their morphologies at high redshift, then it will be difficult to choose adequate samples wisely for comparison with present-epoch cluster ellipticals. The use of WFPC2 imaging to trace the evolution of galaxies divided according to their Hubble types becomes more complicated if morphological classes among galaxies are not conserved. An investigation of the morphological effects of interactions on galaxies in high-redshift clusters, which is beyond the scope of our study but has been explored through simulations by, e.g., Moore et al. (1996), would be necessary to quantify this effect.

Another potential problem with our morphological selection is the lack of distinction we make between E and S0 morphologies. Though apparently similar today in many ways, elliptical and S0 galaxies may also have important differences. If they have followed different evolutionary histories, this may affect conclusions reached from an analysis of their joint photometric properties.

Dressler et al. (1997), using WFPC2 imaging data, have reported evidence for an increase in the proportion of S0 galaxies in clusters from  $z \sim 0.5$  to the present (see also Smail et al. 1997). Recall that we have not attempted to distinguish between elliptical and S0 galaxies in our samples. If the Butcher-Oemler effect were due to disk galaxies evolving to become S0 galaxies between  $z \sim 0.5$  and  $z = 0$ , then this may have some effect on the galaxy colors and color scatter that we observe. On the one hand, if the transformation from spiral to lenticular is accompanied by star formation or is the result of the truncation of star formation in the pre-existing spiral galaxy disks, then “younger” S0 galaxies at higher redshifts should be bluer, affecting both their mean colors and the scatter in those colors. However, at some point, the S0 progenitors would no longer be classified as S0 galaxies on the basis of their morphologies but, rather, as later type disk galaxies instead and thus would “drop out” of our early-type galaxy sample at larger redshifts. The influence of their bluer colors on the mean photometric trends we are studying here would then cease.

We can assess some of these issues in a preliminary way by looking at the fraction of E + S0 galaxies in the cores of



clusters versus redshift. The numbers listed in Table 1 can be used to estimate the ratio of field-corrected early-type cluster galaxies to field-corrected cluster galaxies of all types within three redshift bins:  $0.3 < z < 0.45$ ,  $0.45 < z < 0.65$ , and  $0.65 < z < 0.9$ . Averaging with uniform weight for each cluster, the fraction of early-type to total cluster galaxies is 0.64, 0.78, and 0.69, respectively, for these redshift bins. Averaging with uniform weight for each cluster galaxy within a redshift bin the fractions are 0.61, 0.74, and 0.8. This crude analysis does not reveal the decline in the frequency of early-type galaxies in high-redshift clusters that might be expected if E+S0 galaxies form from mergers of later type galaxies or if S0 galaxies in  $z \sim 0.3$  clusters form from later type spirals at higher redshift. However, it is worth noting that the fraction of early-type galaxies in the Coma Cluster sample used for reference here is 0.96, which again hints at a transition in cluster galaxy properties in the range  $0 < z < 0.3$ .

There is indeed evidence for stellar population differences between elliptical and lenticular galaxies in the local universe. Bothun & Gregg (1990) have used optical-IR photometry of the bulge and disk components of S0 galaxies to show that the disks appear to be younger (more intermediate-age stars) than the bulges. Schweizer & Seitzer (1992) examined the *UBV* color-magnitude relation for E and S0 galaxies separately and found that while the mean slopes and intercepts of the relations were the same (see also Sandage & Visvanathan 1978), the color scatter about the mean is substantially larger for the S0 galaxies. However, it is worth noting that the observational samples for both of these studies consisted primarily of *field* galaxies, and not the inhabitants of the cores of rich clusters. Considering elliptical and S0 galaxies separately in the Coma Cluster data used here for our  $z = 0$  reference sample, De Propris et al. (1998) find little indication of significantly larger scatter in the S0 colors. Nevertheless, it is important to keep in mind that elliptical and S0 galaxies may have followed different evolutionary paths. It would be very interesting to repeat our analysis for samples of distant cluster elliptical and S0 galaxies separately to search for different behavior. This might be accomplished using new, precise morphological catalogs (e.g., Smail et al. 1997). However, the accurate separation of S0 from elliptical galaxies at  $z > 0.5$  using WFPC2 imaging still needs to be carefully investigated.

Even within the traditional, passive evolution scenarios, it is important to consider possible selection effects resulting from the choice of early-type galaxies in clusters as a sample to investigate. Galaxy clusters are rare objects, far out on the high-mass tail of bound structures in the universe. In hierarchical models with  $\Omega = 1$ , this is increasingly true at higher redshifts—massive, bound clusters should be increasingly unusual objects, formed from larger and more extreme peaks in the primordial spectrum of mass fluctuations. Kauffmann (1996) has appealed to this as part of the explanation of the Butcher-Oemler effect, and it may play a role in our understanding of the early-type cluster galaxies as well. In biased galaxy formation scenarios, galaxies in the vicinity of large-scale overdensities may collapse and form earlier than those in less dense regions. It may be that by studying only clusters, we would be increasingly biased toward “old” galaxies at higher redshifts. Indeed, according to Kauffmann & Charlot (1997), this is the reason hierarchical merging models for rich clusters display elliptical galaxy evolution that appears indistinguishable from that predict-

ed by the classical passive scenario. In these models, rich clusters at high redshift formed earlier than clusters with comparable circular velocities today, and correspondingly the star formation and merging histories of their galaxies are pushed back to earlier times. By modeling (or observing) apparently similar clusters at each redshift, one does not trace the continuous evolution of a single collection of galaxies but instead selects only the oldest galaxies at any redshift, which thus mimic passive evolutionary behavior.

A natural consequence of such models would be that the evolution of elliptical galaxies should depend on their environments. Evidence for intermediate-age stellar populations in some elliptical galaxies today (see, e.g., Worthey 1996), which may well correlate with their environment (Bower et al. 1990), would support this idea. Arguing against this, however, is the fact that our distant cluster sample does in fact span a broad range of optical richness and X-ray luminosity and that the observed evolutionary trends seem to be independent of these environmental factors. It is also worth stressing that the hierarchical models of (e.g.) Kauffmann & Charlot (1997) consider only  $\Omega = 1$  CDM universes. In an open universe, structure formation progresses differently, with rich clusters forming earlier and “freezing out” at comparatively high redshift. Presumably, the history of cluster ellipticals in an open universe would also proceed differently and might more closely resemble classical passive evolution across a broader range of environments. Extending the observations presented here, as well as the theoretical models, to early-type galaxies in high-redshift groups and in the field would add another useful dimension to the problem.

## 5. CONCLUSIONS

The color evolution seen in Figure 3 is consistent with the idea that luminous early-type cluster galaxies have evolved with time and that their stellar populations were younger at high redshifts. In itself this is no surprise; it is the uniformity and regularity of the spectrophotometric evolution that is the more important result. The degree of color evolution that we find is mild. At  $z = 0.8$ – $0.9$ , the observed  $R-K$  colors correspond approximately to rest-frame  $U-J$ . Early-type cluster galaxies at that epoch were only 0.4–0.6 mag bluer at these wavelengths than are galaxies of the same morphological types in the Coma Cluster today. Most of this change in color occurs because of an increase in the near-UV flux—the IR-IR colors change very little. The mean ages of the stars in E+S0 galaxies in the distant clusters are thus younger than those in their present-day counterparts, but their intrinsic colors are still quite red out to nearly  $z = 1$ . Spectrophotometric models of passive evolution predict that UV-to-IR color evolution should be rapid during the first  $\sim 2$  Gyr after star formation ceases, quickly reaching red colors that evolve in a slow and steady fashion thereafter. Looking back to  $z = 0.9$  (5.6 Gyr ago for our adopted cosmology), we evidently have not yet closely approached the time at which the bulk of the stars in early-type cluster galaxies were young.

This conclusion is reinforced by the consistently small scatter in the galaxy colors out to  $z = 0.9$ . The rms dispersion in the *blue*– $K$  colors remains fixed at approximately 0.1 mag over the redshift range of our sample, without evidence for the substantial change that might be expected if the early-type cluster galaxies formed over a broad range of redshifts. It is reasonable to expect some component of the

intrinsic color scatter at all redshifts is due to metallicity variations, and that overall the evolution of early-type galaxies within a given cluster is highly synchronized. In addition, we see little evidence of substantial variations in the average galaxy colors from cluster to cluster at a fixed redshift, despite the fact that the clusters span a wide range of richnesses and X-ray luminosities. The constancy with redshift of the slope in the color-magnitude relation of the luminous E + S0 cluster galaxies strongly favors a scenario in which this slope arises from a mass-metallicity correlation, rather than one involving age. It appears that, on average, the evolutionary history of the majority of luminous early-type cluster galaxies has been very similar.

It is important to recall that the redshift dependence of the galaxy colors shown in Figure 3 describes the evolution of the *stellar populations* within those galaxies rather than the evolution of the *galaxies* themselves. The histories of galaxies and of the stars from which they are made may, in principle, differ substantially. It is for this reason that hierarchical merging models, as described in § 1, are able to match the color properties of nearby cluster galaxies, despite the fact that substantial merging takes place at relatively late times. In those models, the bulk of the *stars* that comprise today's elliptical galaxies form early—the assembly of the galaxy itself occurs fairly late. However, this merging is unlikely to occur without some impact on the galaxy colors owing to episodes of star formation during the merging process. In particular, it has often been noted that mergers of disk galaxies cannot produce the high phase-space density of stars observed in the central regions of ellipticals unless some amount of star formation takes place in gas funneled to the nucleus of the merger remnant (see, e.g., Carlberg 1986; Hernquist, Spitzer, & Heyl 1993; Barnes & Hernquist 1996). If most elliptical galaxies in clusters form by a process of late mergers, there should be some detectable signature on their overall photometric properties such as the scatter in their colors or the slope of the color-magnitude relation. By extending the redshift baseline for cluster photometric studies to  $z = 0.9$ , a redshift at which hierarchical models predict that galaxy formation is only partially complete, we have provided a data set against which detailed models can be tested. It seems that it is not difficult to reconcile the observed color evolution with tra-

ditional models of monolithic collapse and passive evolution for early-type galaxies, but it remains to be seen whether other scenarios can account for the observations. In this context, it will be important to examine the luminosity functions of cluster galaxies as a function of redshift and of morphological type, as these should be more sensitive to the merging history of the galaxies than the colors themselves.

The upper redshift limit of our cluster sample just reaches the point at which serious constraints can be placed on the evolutionary history of early-type galaxies. Beyond  $z \sim 1$  in cosmologically flat CDM models, the amount of merging occurring within the prior  $\sim 1$  Gyr is sufficiently large so as to seriously inflate the locus of early-type galaxy colors, even if the recent, merger-induced starbursts are small (Kauffmann 1996). The identification of clusters at  $z > 1$  and the characterization of their galaxy populations should provide a powerful means of testing galaxy formation theories.

The authors would like to thank NOAO for a generous allocation of observing time to this project and the staffs at Kitt Peak and Cerro Tololo for their help with the observing. The referee helped us to improve the final version by providing a valuable critique of the submitted version of this paper. We also thank Marcia Rieke for allowing us to use her unpublished elliptical spectrum, Megan Donahue for allowing us to use her WFPC2 image of MS 1054.5–0321, and the many investigators who originally collected the *HST* data used in our archival program. Stephanie Charlot has provided much advice and guidance concerning the population synthesis models, as well as many interesting discussions about cluster galaxy evolution. Support for this work was provided by NASA through grant number AR-5790.02-94A from the Space Telescope Science Institute, which is operated by the Association of Universities for Research in Astronomy, Inc., under NASA contract NAS 5-26555. Portions of the research described here were carried out by the Jet Propulsion Laboratory, California Institute of Technology, under a contract with NASA. Work performed at the Lawrence Livermore National Laboratory is supported by the DOE under contract W7405-ENG-48.

## REFERENCES

- Aragón-Salamanca, A., Ellis, R. S., Couch, W. J., & Carter, D. 1993, *MNRAS*, 248, 128.  
 Arimoto, N., & Yoshii, Y. 1987, *A&A*, 173, 23.  
 Barger, A., Aragón-Salamanca, A., Ellis, R. S., Couch, W. J., Smail, I., & Sharples, R. 1997, *MNRAS*, 279, 1.  
 Barnes, J. E., & Hernquist, L. 1996, *ApJ*, 471, 115.  
 Beers, T. C., Flynn, K., & Gebhardt, K. 1990, *AJ*, 100, 32.  
 Belloni, P., et al. 1998, in preparation.  
 Bender, R., Burstein, D., & Faber, S. 1993, *ApJ*, 411, 153.  
 Bothun, G., & Gregg, M. 1990, *ApJ*, 350, 73.  
 Bower, R., Ellis, R. S., Rose, J. A., & Sharples, R. M. 1990, *AJ*, 99, 530.  
 Bower, R., Lucey, J. R., & Ellis, R. S. 1992, *MNRAS*, 254, 589.  
 Bruzual A., G., & Charlot, S. 1993, *ApJ*, 405, 538.  
 ———. 1996, unpublished (BC96).  
 Burstein, D., & Heiles, C. 1982, *AJ*, 87, 1165.  
 Butcher, H., & Oemler, A., Jr. 1978, *ApJ*, 219, 18.  
 Caldwell, N., & Rose, J. A. 1997, *AJ*, 113, 492.  
 Caldwell, N., Rose, J. A., Sharples, R. M., Ellis, R. S., & Bower, R. G. 1993, *AJ*, 106, 473.  
 Carlberg, R. 1986, *ApJ*, 310, 593.  
 Charlot, S., & Silk, J. 1994, *ApJ*, 432, 453.  
 Charlot, S., Worthey, G., & Bressan, A. 1996, *ApJ*, 457, 625.  
 Cole, S., Aragón-Salamanca, A., Frenk, C. S., Navarro, J. F., & Zepf, S. E. 1994, *MNRAS*, 271, 781.  
 Couch, W. J., Ellis, R. S., Sharples, R. M., & Smail, I. 1994, *ApJ*, 430, 121.  
 Couch, W. J., & Sharples, R. M. 1987, *MNRAS*, 229, 423.  
 De Propris, R., Eisenhardt, P. R. M., Stanford, S. A., & Dickinson, M. 1998, in preparation.  
 Dickinson, M. 1995, in *ASP Conf. Proc. 86, Fresh Views of Elliptical Galaxies*, ed. A. Buzzoni, A. Renzini, & A. Serrano (San Francisco: ASP), 283.  
 ———. 1997, in *Galaxy Scaling Relations: Origins, Evolution, and Applications*, ed. L. da Costa (Berlin: Springer), in press.  
 Dickinson, M., & Broadhurst, T. 1998, in preparation.  
 Djorgovski, S. G., et al. 1995, *ApJ*, 438, 13.  
 Dokkum, P., & Franx, M. 1996, *MNRAS*, 281, 985.  
 Dressler, A., & Gunn, J. 1983, *ApJ*, 270, 7.  
 ———. 1990, in *Evolution of the Universe of Galaxies*, ed. R. Kron (Dordrecht: Kluwer), 200.  
 ———. 1992, *ApJS*, 78, 1.  
 Dressler, A., et al. 1997, *ApJ*, 490, 577.  
 Dressler, A., Oemler, A., Sparks, B., & Lucas, R. 1994, *ApJ*, 435, 23.  
 Driver, S. P., Windhorst, R. A., Ostrander, E. J., Keel, W. C., Griffiths, R. E., & Ratnatunga, K. A. 1995, *ApJ*, 449, 23.  
 Eggen, O. J., Lynden-Bell, D., & Sandage, A. R. 1962, *ApJ*, 136, 748 (ELS).  
 Eisenhardt, P. R. M., et al. 1998, in preparation.  
 Ellis, R. S., Smail, I., Dressler, A., Couch, W. J., Oemler, A., Butcher, H., & Sharples, R. M. 1997, *ApJ*, 483, 582.

- Elston, R., Eisenhardt, P., & Stanford, S. A. 1998, in preparation
- Franx, M., & Illingworth, G. 1990, *ApJ*, 359, 41
- Frogl, J., Persson, E., Aaronson, M., & Matthews, K. 1978, *ApJ*, 220, 75
- Glazebrook, K., Ellis, R., Santiago, B., & Griffiths, R. 1995, *MNRAS*, 275, 19
- Hernquist, L., Spergel, D. N., & Heyl, J. S. 1993, *ApJ*, 416, 415
- Holtzman, J. A., Burrows, C. J., Casertano, S., Hester, J. J., Trauger, J. T., Watson, A. M., & Worthey, G. 1995, *PASP*, 107, 1065
- Johnson, H. L. 1966, *ApJ*, 143, 187
- Kauffmann, G. 1996, *MNRAS*, 281, 487
- Kauffmann, G., & Charlot, S. 1997, *astro-ph/9704148*
- Kauffmann, G., White, S. D. M., & Guiderdoni, B. 1993, *MNRAS*, 264, 201
- Kodama, T., & Arimoto, N. 1997, *A&A*, 320, 41
- Larson, R. J. 1974, *MNRAS*, 169, 229
- Lilly, S. J. 1987, *MNRAS*, 229, 573
- Lubin, L. 1996, *AJ*, 112, 23
- Mathis, J. 1990, *ARA&A*, 28, 37
- Moore, B., Katz, N., Lake, G., Dressler, A., & Oemler, A. 1996, *Nature*, 379, 613
- O'Connell, R. W. 1980, *ApJ*, 236, 340
- Oemler, A., Jr., Dressler, A., & Butcher, H. R. 1997, *ApJ*, 474, 561
- Pahre, M. A., Djorgovski, S. G., & De Carvalho, R. R. 1996, *ApJ*, 456, 79
- Rakos, K. D., & Schombert, J. 1995, *ApJ*, 439, 47
- Sandage, A. R., & Visvanathan, N. 1978, *ApJ*, 223, 707
- Schweizer, F., & Seitzer, P. 1988, *ApJ*, 328, 88
- . 1992, *AJ*, 104, 1039
- Schweizer, F., Seitzer, P., Faber, S. M., Burstein, D., Dalle Ore, C. M., & Gonzalez, J. J. 1990, *ApJ*, 364, 33.
- Searle, L., Sargent, W. L. W., & Bagnuolo, W. G. 1973, *ApJ*, 179, 427
- Smail, I., Dressler, A., Couch, W. J., Ellis, R. S., Oemler, A., Butcher, H., & Sharples, R. M. 1997, *ApJS*, 110, 213
- Stanford, S. A., Eisenhardt, P. R. M., & Dickinson, M. E. 1995, *ApJ*, 450, 512 (SED95)
- Stanford, S. A., et al. 1998, in preparation
- Tinsley, B. M., & Gunn, J. E. 1976, *ApJ*, 203, 52
- Toomre, A. 1978, in *Evolution of Galaxies and Stellar Populations*, ed. B. M. Tinsley & R. Larson, R. (New Haven: Yale Univ. Press), 401
- Valdes, F. 1982, *Proc. SPIE*, 331, 465
- White, S. D. M., & Frenk, C. S. 1991, *ApJ*, 379, 52
- Wirth, G. D., Koo, D. C., & Kron, R. 1994, *ApJ*, 435, 105
- Worthey, G. 1996, *astro-ph/9611180*
- Ziegler, B., & Bender, R. 1997, *astro-ph/9704280*